

Higgs Gravitational Interaction, Weak Boson Scattering, and Higgs Inflation in Jordan and Einstein Frames

Jing Ren,^a Zhong-Zhi Xianyu,^{a,b} Hong-Jian He^{a,c,d}

^aInstitute of Modern Physics and Center for High Energy Physics,
Tsinghua University, Beijing 100084, China

^bTheoretical Particle Physics and Cosmology Group, Department of Physics,
King's College London, London WC2R 2LS, UK

^cCenter for High Energy Physics, Peking University, Beijing 100871, China

^dKavli Institute for Theoretical Physics China, CAS, Beijing 100190, China

E-mail: jingren2004@gmail.com, xianyuzhongzhi@gmail.com,
hjhe@tsinghua.edu.cn

Abstract.

We study gravitational interaction of Higgs boson through the unique dimension-4 operator $\xi H^\dagger H \mathcal{R}$, with H the Higgs doublet and \mathcal{R} the Ricci scalar curvature. We analyze the effect of this dimensionless nonminimal coupling ξ on weak gauge boson scattering in both Jordan and Einstein frames. We explicitly establish the longitudinal-Goldstone boson equivalence theorem with nonzero ξ coupling in both frames, and analyze the unitarity constraints. We study the ξ -induced weak boson scattering cross sections at $\mathcal{O}(1 - 30)$ TeV scales, and propose to probe the Higgs-gravity coupling via weak boson scattering experiments at the LHC (14 TeV) and the next generation pp colliders (50 – 100 TeV). We further extend our study to Higgs inflation, and quantitatively derive the perturbative unitarity bounds via coupled channel analysis, under large field background at the inflation scale. We analyze the unitarity constraints on the parameter space in both the conventional Higgs inflation and the improved models in light of the recent BICEP2 data.

Keywords:

Particle physics - Cosmology connection, Inflation, Quantum gravity phenomenology,
Cosmology of theories beyond the SM

Contents

1	Introduction	2
2	Higgs-Gravity Interactions in Jordan and Einstein Frames	6
2.1	Higgs-Gravity Interactions in Jordan Frame	6
2.2	Higgs-Gravity Interactions in Einstein Frame	8
3	Weak Boson Scattering in Jordan and Einstein Frames	11
3.1	Analysis in Jordan Frame	12
3.2	Analysis in Einstein Frame	16
3.3	Perturbative Unitarity Bound on Higgs-Gravity Coupling	19
3.4	Probing Higgs-Gravity Coupling via Weak Boson Scattering	22
4	Unitarity Analysis for Higgs Inflation	25
4.1	Background-Dependent Formulation	26
4.2	Analysis of Scattering Amplitudes in Large Field Background	26
4.3	Unitarity Constraints for Higgs Inflation	28
5	Conclusions	33
A	Feynman Rules in Jordan and Einstein Frames	35
A.1	Feynman Rules in Jordan Frame	35
A.2	Feynman Rules in Einstein Frame	36
	References	38

1 Introduction

The LHC discovery of a Higgs boson (~ 125 GeV) [1, 2] has begun a new era for particle physics and its interface with cosmology and gravitation research. The Higgs boson plays a distinctive role in the standard model (SM) of particle physics. It is the only fundamental scalar particle in the SM. It spontaneously breaks the electroweak gauge symmetry and provides the origin of inertial masses for all massive particles: weak gauge bosons, quarks, leptons and neutrinos. As measured from the current LHC experiments [2], the properties of this 125 GeV new particle (including its signal strengths in several decay channels and its spin/parity) are still compatible with the SM predictions. However, most of its couplings (especially its Yukawa couplings and self-couplings) have not yet been tested, and possible new physics can cause deviations of these couplings from those of the SM Higgs boson, which will be probed at the upcoming LHC runs and the future e^+e^- and pp colliders [3].

Furthermore, the SM is apparently incomplete for not containing the gravitational force, despite all SM particles join in gravitation. Even though the Einstein general relativity (GR) still gives the best description of gravitation, it is a notoriously nonrenormalizable field theory [4]. Hence, it is compelling to incorporate the SM and GR together as a joint low energy effective theory below the Planck scale, and explore the testable effects from this unavoidable interface. Especially, with the LHC Higgs discovery [1, 2], we are strongly motivated to study gravitational interactions of the Higgs boson, because the Higgs boson generates inertial masses for all SM particles while the gravity force arises from their gravitational masses.

Such an effective theory always has an ultraviolet (UV) cutoff, at or below the Planck mass. In this formulation, one can write down the most general action under all known symmetries, as a series of effective operators with increasing mass-dimensions and with proper suppressions by the UV cutoff [5]. Thus, for the experimentally accessible energy ranges being well below the UV cutoff, the leading terms of this effective action can provide a fairly good approximation of the full theory.

In fact, under the $U(1)_Y \otimes SU(2)_L \otimes SU(3)_c$ gauge symmetries and given the three families of leptons and quarks, the SM Lagrangian is already the most general effective theory up to dimension-4 operators. On the other hand, the Einstein-Hilbert action of general relativity represents the leading terms of mass-dimension zero and two, under the generally covariant expansion,

$$S_{\text{EH}} = M_{\text{Pl}}^2 \int d^4x \sqrt{-g} \left(-\Lambda + \frac{1}{2} \mathcal{R} \right), \quad (1.1)$$

where $M_{\text{Pl}} = (8\pi G)^{-1/2} \simeq 2.44 \times 10^{18}$ GeV gives the reduced Planck mass, Λ denotes the cosmological constant, and \mathcal{R} is the Ricci scalar. One can continue to write down more operators with higher mass-dimensions in this series. Up to dimension-4, we have

$$S_{\text{G4}} = \int d^4x \sqrt{-g} (c_1 \mathcal{R}^2 + c_2 \mathcal{R}_{\mu\nu} \mathcal{R}^{\mu\nu}). \quad (1.2)$$

There is another possible term $\mathcal{R}_{\mu\nu\rho\sigma} \mathcal{R}^{\mu\nu\rho\sigma}$ allowed by the symmetry, but is not independent up to integration by parts.

In the GR, the gravitational interactions of matter fields (including all the SM particles) are introduced in the manner of minimal coupling. In this way, the fluctuation of spacetime metric couples to matter fields through the energy-momentum tensor,

$$S_{\text{MC}} = - \int d^4x \sqrt{-g} \delta g_{\mu\nu} T_{\text{SM}}^{\mu\nu}, \quad (1.3)$$

where the energy-momentum tensor $T_{\text{SM}}^{\mu\nu}$ contains the SM fields. For bosonic fields, the rule of minimal coupling is practically equivalent to making two replacements in the SM Lagrangians. One is to replace Minkowski metric by a general metric $\eta_{\mu\nu} \rightarrow g_{\mu\nu}$ (together

with the rescaling of integral measure $d^4x \rightarrow d^4x \sqrt{-g}$). The other is to replace the partial derivative by covariant derivative $\partial_\mu \rightarrow \nabla_\mu$, where ∇_μ is adapted for $g_{\mu\nu}$ with $\nabla_\lambda g_{\mu\nu} = 0$. For fermionic fields, the vierbein and spin connection are introduced. With these, we could conclude that the joint action $S_{\text{EH}} + S_{\text{G4}} + S_{\text{MC}}$ provides an effective description of the SM with gravitation. But, this action is incomplete up to dimension-4 operators. There is a unique dimension-4 operator which couples the Higgs doublet H to the scalar curvature R , and thus should be added to the above action,

$$S_{\text{NMC}} = \int d^4x \sqrt{-g} \xi \mathcal{R} H^\dagger H, \quad (1.4)$$

where ξ is a dimensionless coupling. This term is conventionally called nonminimal coupling term since it does not follow the rule of minimal coupling. We note that up to dimension-4 operators, the nonminimal coupling could only appear for the spin-0 field. This fact adds a unique feature to the Higgs boson in the SM.

Hence, the complete Lagrangian up to dimension-4 operators and joining both the SM and GR should take the following form,

$$S = S_{\text{EH}} + S_{\text{G4}} + S_{\text{MC}} + S_{\text{NMC}}. \quad (1.5)$$

The non-minimal coupling term S_{NMC} is generally covariant and respects all known symmetries of the SM. We further note that $\xi \rightarrow 0$ does not enlarge the symmetry, and a nonzero ξ will still be generated by loop diagrams even if one sets $\xi = 0$ classically [6]. Another special value is the conformal coupling $\xi = -1/6$, which makes the theory Weyl-invariant for massless scalar field. But, the SM Higgs doublet is not massless, and the Weyl symmetry (which reduces to the conformal symmetry in flat spacetime) is also not a symmetry of the SM. All these facts imply that the size of this dimensionless nonminimal coupling ξ can be rather large *a priori*. In fact, a large ξ around the order of 10^4 has been put in use for the Higgs inflation models [7–13] in which the Higgs boson is responsible for two distinctive physical processes, namely, it drives inflation at a typically very high inflation scale, and triggers the electroweak symmetry breaking at weak scale.¹

Recently, Ref. [14] derived an interesting bound on ξ from the LHC Higgs data, by assuming the 125 GeV boson to be the SM Higgs boson. As will be shown in Sec. 2, a large ξ will cause a universal suppression of the Higgs boson coupling with all other SM particles. Thus, using the measured Higgs signal strengths in 2012, Ref. [14] derived an upper bound, $|\xi| < 2.6 \times 10^{15}$. Furthermore, in the recent study [15], we derived the perturbative unitarity bound on ξ by analyzing the coupled-channel longitudinal weak boson scattering under flat

¹ Ref. [8] first observed that the value of Higgs boson mass can be directly related to the CMB parameters in the Higgs inflation.

spacetime background, and we demonstrated the longitudinal-Goldstone boson equivalence theorem [16] in the presence of ξ coupling. In [15], we did calculations only in Einstein frame, where the nonminimal coupling is transformed away by redefining the metric tensor. But, we may also perform the analysis in Jordan frame, i.e., with the field variables written in the action (1.5). The physical (in)equivalence between Jordan frame and Einstein frame is a subtle issue which still lacks a full consensus (especially at the quantum level) [10, 11, 17–19]. Then, it is desirable to perform an independent analysis within the Jordan frame, in comparison with our previous Einstein frame analysis [15]. In this paper, we will show that the same results can be inferred from Jordan frame with a fully different set of Feynman rules (Appendix A). This serves as a valuable consistency check of our analysis. For the first time, we will further explicitly prove the longitudinal-Goldstone equivalence theorem with nonzero ξ in Jordan frame. It provides another nontrivial consistency check on our Jordan-frame analysis.

There are some discussions on the unitarity issue with the nonminimal coupling for the purpose of Higgs inflation models [20]. People usually applied power-counting arguments to get the scalar or vector boson scattering amplitudes, and estimate the allowed regime for the perturbative calculations of Higgs inflation. At the first sight, the unitarity bound is around M_{Pl}/ξ for $\xi \gg 1$, which is lower than the typical inflation scale $M_{\text{Pl}}/\sqrt{\xi}$. Later studies [12, 13] suggested that unitarity bounds vary with respect to classical background of inflaton field. Considering this background dependence, the unitarity bound is expected to be relaxed to $O(M_{\text{Pl}}/\sqrt{\xi})$ in the inflationary era. This implies that the perturbative analysis of inflation dynamics and primordial fluctuation would be reliable. These discussions are suggestive, but are only qualitative power-counting estimates with different focus and context. In this paper, we will systematically extend our analysis to quantitatively derive the unitarity constraints for a generical Higgs inflaton background. We will consider the conventional Higgs inflation [7] and the improved models [21–23] in light of the recent BICEP2 data [24].

This paper is organized as follows. In Sec. 2, we will outline the formulation with nonminimal coupling for the Jordan and Einstein frames. In Sec. 3, we study the longitudinal weak boson scatterings in both frames. This gives a systematical extension of our previous short study [15] which was for the Einstein frame alone and at the lowest order of $1/M_{\text{Pl}}^2$. In Sec. 3.3, we quantitatively derive the perturbative unitarity bound on the Higgs-curvature coupling ξ in both the electroweak vacuum and the large field background. We further study ξ -dependent weak boson scattering cross sections at the scales of $\mathcal{O}(1 - 30)\text{TeV}$ energies, which serve as the new probes of ξ at the upcoming LHC (14 TeV) and the future high energy pp colliders (50 – 100 TeV) [25]. In Sec. 4, we systematically extend our analysis to the Higgs inflation models in the large field background. We conclude in Sec. 5. Finally, we

present the necessary Feynman rules for both Jordan and Einstein frames in Appendix A.

2 Higgs-Gravity Interactions in Jordan and Einstein Frames

In this section, we discuss the formulation for the nonminimal gravitational coupling of the SM Higgs doublet, which will serve as the base for our systematical studies in the following sections 3–4. The set of field variables that manifests this nonminimal coupling (1.4) is conventionally called Jordan frame, which is part of the joint effective action (1.5). One can make a proper Weyl transformation on the metric tensor, under which the nonminimal coupling term (1.4) is fully transformed away. This new metric is usually called Einstein frame, in which the original Einstein equation of GR holds. For clarity we will use a superscript (J) to label the Jordan frame metric and other geometric quantities, while the Einstein frame quantities are presented without superscript so long as they appear confusion-free.

2.1 Higgs-Gravity Interactions in Jordan Frame

By definition, the action in Jordan frame takes the form of (1.5). Hence, the nonminimal coupling term $\xi \mathcal{R}^{(J)} H^\dagger H$ is manifest in Jordan frame. To analyze the gravitational interactions of Higgs boson and weak gauge bosons, we extract from (1.5) the terms with scalar-curvature, weak gauge bosons and Higgs doublet, and organize them in a more transparent way,

$$S_J = \int d^4x \sqrt{-g^{(J)}} \left[\left(\frac{1}{2} M^2 + \xi H^\dagger H \right) \mathcal{R}^{(J)} - \sum_j \frac{1}{4} F_{\mu\nu j}^a F_j^{\mu\nu a} + (D_\mu H)^\dagger (D^\mu H) - V(H) \right], \quad (2.1)$$

where $\mathcal{R}^{(J)}$ is the Ricci scalar associated with the Jordan frame metric $g_{\mu\nu}^{(J)}$, and $F_{\mu\nu i}^a = (W_{\mu\nu}^a, B_{\mu\nu})$ are gauge field strengths of the electroweak gauge group $SU(2)_L \otimes U(1)_Y$. In this action we do not display the cosmological constant term as well as the dimension-4 operators of pure gravity, since they are irrelevant to the current study. The Higgs doublet H is parameterized as, $H = (\pi^+, \frac{1}{\sqrt{2}}(v + \hat{\phi} + i\pi^0))^T$ and has the potential $V(H) = \lambda (H^\dagger H - \frac{1}{2}v^2)^2$. The potential reaches its minimum when Higgs doublet acquires a nonzero vacuum expectation value (VEV), $\langle H \rangle = \frac{1}{\sqrt{2}}(0, v)^T$. Substituting this VEV into the action (2.1), we see that the nonminimal coupling term gives a contribution to the pure gravitational term $\sqrt{-g^{(J)}} \mathcal{R}^{(J)}$, and leads to an effective Einstein-Hilbert action,

$$\int d^4x \sqrt{-g^{(J)}} \left(\frac{1}{2} M^2 + \xi H^\dagger H \right) \mathcal{R}^{(J)} \supset \int d^4x \sqrt{-g^{(J)}} \frac{1}{2} (M^2 + \xi v^2) \mathcal{R}^{(J)}. \quad (2.2)$$

Thus, we identify the coefficient, $M^2 + \xi v^2 = M_{\text{Pl}}^2$, to reproduce the correct Newton constant.

In Jordan frame, gravitons make important contributions to the weak gauge boson scattering amplitudes. Hence, we perturb the metric, $g_{\mu\nu}^{(J)} = \bar{g}_{\mu\nu}^{(J)} + \kappa \hat{h}_{\mu\nu}$, with the background value $\bar{g}_{\mu\nu}^{(J)}$ identified as the flat Minkowski metric, $\bar{g}_{\mu\nu}^{(J)} = \eta_{\mu\nu}$. The perturbation coupling $\kappa = \sqrt{2}M_{\text{Pl}}^{-1}$ is chosen such that the spin-2 component in $\hat{h}_{\mu\nu}$ has the correct normalization. A special feature of the Jordan frame is that both the perturbed metric $\hat{h}_{\mu\nu}$ and the Higgs field $\hat{\phi}$ are not canonically normalized due to kinetic mixings. To see this, we inspect the kinetic terms for $\hat{h}_{\mu\nu}$ and $\hat{\phi}$ from (2.1),

$$S_J \supset \frac{1}{4} (\hat{h} \square \hat{h} - \hat{h}^{\mu\nu} \square \hat{h}_{\mu\nu} + 2\hat{h}_{\mu\lambda} \partial^\mu \partial_\nu \hat{h}^{\nu\lambda} - 2\hat{h} \partial^\mu \partial^\nu \hat{h}_{\mu\nu}) - \frac{1}{2} \hat{\phi} \square \hat{\phi} + \xi \kappa v \hat{\phi} (\square \hat{h} - \partial^\mu \partial^\nu \hat{h}_{\mu\nu}), \quad (2.3)$$

where $\hat{h} \equiv \hat{h}^\mu{}_\mu$. Thus, we define another set of canonically normalized fields $h_{\mu\nu}$ and ϕ ,

$$\hat{h}_{\mu\nu} = h_{\mu\nu} - \eta_{\mu\nu} \xi \kappa v \zeta \phi, \quad \hat{\phi} = \zeta \phi, \quad (2.4)$$

with the rescaling factor,

$$\zeta \equiv (1 + 3\xi^2 \kappa^2 v^2)^{-\frac{1}{2}} = (1 + 6\xi^2 v^2 / M_{\text{Pl}}^2)^{-\frac{1}{2}}. \quad (2.5)$$

After this field rescaling, we readily verify that both new variables $h_{\mu\nu}$ and ϕ are canonically normalized, with the correct kinetic term,

$$\mathcal{L}_{\text{kin}} = \frac{1}{4} (h \square h - h^{\mu\nu} \square h_{\mu\nu} + 2h_{\mu\lambda} \partial^\mu \partial_\nu h^{\nu\lambda} - 2h \partial^\mu \partial^\nu h_{\mu\nu}) - \frac{1}{2} \phi \square \phi. \quad (2.6)$$

The above field redefinitions have two general consequences. First, from the rescaling of Higgs field $\hat{\phi} = \zeta \phi$, we see that all SM couplings of gauge fields and fermions to the Higgs boson ϕ receive a universal rescaling factor ζ associated with each Higgs field in the vertex. This rescaling factor $\zeta < 1$ causes a universal suppression on the Higgs boson couplings with all other SM particles. Second, the original perturbed metric $\hat{h}_{\mu\nu}$ contains a portion of canonical Higgs field ϕ . Hence, there will be new Higgs couplings to other SM particles which are induced from gravitational interactions. Since the graviton $\hat{h}_{\mu\nu}$ couples to matter fields through their stress tensor (with the exception of nonminimal coupling to Higgs doublet), the graviton-induced Higgs couplings to SM particles are all suppressed by the small parameter κ . But, as we will show, the gravity contributions can be significant when the nonminimal coupling ξ is large.

To compute scattering amplitudes with graviton exchange, we fix the gauge symmetry of linearized general covariance by choosing the harmonic gauge. This amounts to adding the gauge-fixing term,

$$\mathcal{L}_{\text{GF}} = \frac{1}{2\alpha} (\partial^\lambda h_{\lambda\mu} - \frac{1}{2} \partial_\mu h)^2, \quad (2.7)$$

with α as the gauge parameter. Then, the kinetic term of the graviton can be inverted to give the graviton propagator,

$$G_{\mu\nu,\rho\sigma}^{(h)}(p) = \frac{i}{p^2 + i\epsilon} \left[2\eta_{\mu(\rho}\eta_{\sigma)\nu} - \eta_{\mu\nu}\eta_{\rho\sigma} - (1-\alpha)\frac{4p_{(\mu}\eta_{\nu)(\rho}p_{\sigma)}}{p^2} \right]. \quad (2.8)$$

The gauge-invariance of the scattering amplitudes can be checked by showing that the α -dependent pieces vanish. This is necessarily true if the graviton is coupled to external on-shell particles, which are subjected to the energy-momentum conservation $\partial^\mu T_{\mu\nu} = 0$ in the flat spacetime. We note that the nonminimal coupling term will spoil the covariant conservation of $T_{\mu\nu}$ with curved background, but it does not affect the flat-space conservation law, $\partial^\mu T_{\mu\nu} = 0$, since the Ricci scalar vanishes in this case.

The relevant new interactions involving canonically normalized graviton $h_{\mu\nu}$ and Higgs ϕ can be extracted from the action (2.1),

$$\Delta\mathcal{L}_{\text{int}}^{h\phi} = \kappa (h_{\mu\nu} - \eta_{\mu\nu}\xi\kappa v\zeta\phi) T^{\mu\nu}, \quad (2.9)$$

where $T^{\mu\nu}$ is the energy-momentum tensor of matter fields, including gauge bosons and Higgs doublet for the current study. In the Feynman-'t Hooft gauge, we have

$$\begin{aligned} T^{\mu\nu} = & \sum_j \left(F_j^{\mu\lambda a} F_{\lambda j}^{\nu a} + \frac{1}{4} g^{\mu\nu} F_{\rho\sigma j}^a F_j^{\rho\sigma a} \right) + m_W^2 \left(W^{\mu a} W^{\nu a} - \frac{1}{2} g^{\mu\nu} W_\lambda^a W^{\lambda a} \right) \\ & + \partial^\mu \pi^a \partial^\nu \pi^a + \partial^\mu \phi \partial^\nu \phi - \frac{1}{2} g^{\mu\nu} \left((\partial_\lambda \pi^a)^2 + (\partial_\lambda \phi)^2 - m_W^2 \pi^a \pi^a - m_\phi^2 \phi^2 \right), \end{aligned} \quad (2.10)$$

where we only keep contributions from kinetic terms and mass terms for the current purpose. We have also set the weak mixing angle $\theta_W = 0$ for simplicity, and dropped terms from the gauge-fixing and Faddeev-Popov ghosts which are irrelevant to the tree-level processes in the present work.

2.2 Higgs-Gravity Interactions in Einstein Frame

The Einstein frame is realized by the field redefinition, $g_{\mu\nu}^{(E)} = \Omega^2 g_{\mu\nu}^{(J)}$, with

$$\Omega^2 = \frac{M^2 + 2\xi H^\dagger H}{M_{\text{Pl}}^2}. \quad (2.11)$$

We see that this field redefinition takes the form of Weyl transformation, and the Weyl factor Ω^2 depends on spacetime coordinates through its dependence on the Higgs-doublet-bilinear term $H^\dagger H$. This transformation is also known as ‘‘conformal transformation’’ in the literature of general relativity. (Here we avoid the use of this terminology since it is also used for a special type of spacetime coordinate transformations that leave the metric invariant up to a spacetime-dependent factor.) We note that the field redefinition here is

not generated by a spacetime coordinate transformation. Hence, one would not expect that the physics described by these two frames to be equivalent *a priori*, as extensively discussed in the literature [10, 11, 17–19]. Thus, in a given study, one should be careful to check whether the two frames describe the same physics or which frame has a better use. But, this ambiguity is absent for our current study of gauge boson scattering processes. As will be explained below, one can always set the background spacetime metric to be flat to a good approximation, and the two “frames” just correspond to different choices of field variables and thus should yield the same physical results.

Let us convert the Jordan frame action (2.1) into the Einstein frame. To achieve this, we note that the Weyl transformation of Ricci scalar takes the form,

$$\mathcal{R}^{(J)} = \Omega^2 \left[\mathcal{R} - 6g^{\mu\nu} \nabla_\mu \nabla_\nu \log \Omega + 6g^{\mu\nu} (\nabla_\mu \log \Omega) (\nabla_\nu \log \Omega) \right], \quad (2.12)$$

where the unlabeled quantities on the right-hand side, such as Ricci scalar \mathcal{R} , the covariant derivative ∇_μ , are associated with the Einstein frame metric $g_{\mu\nu} = g_{\mu\nu}^{(E)}$. We drop the superscript (E) for these quantities to simplify the notation. Substituting this transformation into (2.1), we obtain the Einstein frame action,

$$S_E = \int d^4x \sqrt{-g} \left[\frac{1}{2} M_{\text{Pl}}^2 \mathcal{R} - \sum_j \frac{1}{4} F_{\mu\nu j}^a F_j^{\mu\nu a} - \frac{3\xi}{\Omega^2} \nabla^2 (H^\dagger H) + \frac{9\xi^2}{M_{\text{Pl}}^2 \Omega^4} (\nabla_\mu (H^\dagger H))^2 + \frac{1}{\Omega^2} (D_\mu H)^\dagger (D^\mu H) - \frac{1}{\Omega^4} V(H) \right]. \quad (2.13)$$

In comparison with the Jordan frame action (2.1), we see that the nonminimal coupling term $\xi \mathcal{R}^{(J)} H^\dagger H$ is fully transformed away. In consequence, the equation of motion (from varying the metric) reproduces the conventional Einstein equation, and the graviton has the correct kinetic term as in the GR. Under the linearized expansion $g_{\mu\nu} = \bar{g}_{\mu\nu} + \kappa h_{\mu\nu}$, we can write the Weyl transformation $g_{\mu\nu} = \Omega^2 g_{\mu\nu}^{(J)}$ in the perturbative form,

$$\begin{aligned} \bar{g}_{\mu\nu} + \kappa h_{\mu\nu} &= \left(1 + \frac{\xi}{M_p^2} 2v\hat{\phi} + \dots \right) (\eta_{\mu\nu} + \kappa \hat{h}_{\mu\nu}), \\ \bar{g}_{\mu\nu} &= \eta_{\mu\nu}, \quad h_{\mu\nu} = \hat{h}_{\mu\nu} + \eta_{\mu\nu} \xi \kappa v \hat{\phi}, \end{aligned} \quad (2.14)$$

where the background in Einstein frame is flat as well. Since Ω^2 contains the Higgs-doublet-bilinear term $H^\dagger H$, new interactions with Higgs fields are induced, where the Higgs field $\hat{\phi}$ is not normalized canonically. With the flat spacetime background $\bar{g}_{\mu\nu} = \eta_{\mu\nu}$ and substituting $H = (\pi^+, \frac{1}{\sqrt{2}}(v + \hat{\phi} + i\pi^0))^T$ into the action (2.13), we derive the following kinetic term (up to bilinear fields) for the Higgs and Goldstone bosons,

$$\mathcal{L}_{\text{kin}} = \frac{1}{2} \left(1 + \frac{6\xi^2 v^2}{M_{\text{Pl}}^2} \right) (\partial_\mu \hat{\phi})^2 + \partial_\mu \pi^- \partial^\mu \pi^+ + \frac{1}{2} (\partial_\mu \pi^0)^2. \quad (2.15)$$

As is clear, to normalize the Higgs kinetic term requires a field redefinition, $\hat{\phi} = \zeta\phi$, where the rescaling factor $\zeta = (1 + 6\xi^2 v^2/M_{\text{Pl}}^2)^{-1/2}$ takes the same form as in the Jordan frame. As compared to (2.4)-(2.6) in the Jordan frame, we see that the canonical Higgs fields in both frames are defined in the same way up to quadratic terms. Thus, we can directly infer the tree-level Higgs mass, $m_\phi^2 = 2\lambda v^2 \zeta^2$, and all the Higgs couplings in the SM under the rescaling for each Higgs field ($\hat{\phi} = \zeta\phi$). For the Higgs self-couplings, we have further contributions from higher dimensional operators besides the rescaling of ζ . These new couplings contain derivatives, so we expect them to become important for scattering processes at high energies. This means that for the present study of the high energy scattering of weak gauge bosons, we should take all these ξ -corrections into account. To the $\mathcal{O}(M_{\text{Pl}}^{-2})$, we extract these new interactions from the action (2.13),

$$\begin{aligned} \Delta\mathcal{L}_{\text{int}}^{ss} = & -\frac{\xi}{2M_{\text{Pl}}^2} \left(|\partial_\mu\pi|^2 + \zeta^2(\partial_\mu\phi)^2 \right) \left(|\pi|^2 + \zeta^2\phi^2 + 2v\zeta\phi \right) \\ & -\frac{3\xi^2}{4M_{\text{Pl}}^2} \left(|\pi|^2 + \zeta^2\phi^2 + 2v\zeta\phi \right) \partial^2 \left(|\pi|^2 + \zeta^2\phi^2 + 2v\zeta\phi \right), \end{aligned} \quad (2.16)$$

where $|\pi|^2 = 2\pi^+\pi^- + (\pi^0)^2$ and $|\partial_\mu\pi|^2 = 2\partial_\mu\pi^+\partial^\mu\pi^- + (\partial_\mu\pi^0)^2$. For the Higgs couplings with weak gauge bosons, we infer,

$$\Delta\mathcal{L}_{\text{int}}^{\phi g} = (2m_W^2 W_\mu^+ W^{\mu-} + m_Z^2 Z_\mu^2) \left[\left(1 - \frac{\xi v^2}{M_{\text{Pl}}^2} \right) \frac{\zeta}{v} \phi + \left(1 - \frac{5\xi v^2}{M_{\text{Pl}}^2} \right) \frac{\zeta^2}{2v^2} \phi^2 \right]. \quad (2.17)$$

For completeness, we further inspect the fermion sector under the present formalism. For Dirac fermion Ψ in the curved background, we can write its kinetic term,

$$S_f = \int d^4x \det(e_\nu^a) \bar{\Psi} \gamma^p e_p^\mu \left(i\partial_\mu - \frac{1}{2} \omega_\mu^{mn} \sigma_{mn} \right) \Psi, \quad (2.18)$$

where e_ν^a and ω_μ^{mn} are vierbein and spin-connection, and $\sigma_{mn} = \frac{i}{2}[\gamma_m, \gamma_n]$. We identify the background to be the Jordan frame, which is related to the flat Einstein frame by $g_{\mu\nu}^{(J)} = \Omega^{-2} \eta_{\mu\nu}$. Then, we can derive expressions for the vierbein and spin-connection in terms of Weyl factor Ω ,

$$e_\mu^m = \Omega^{-1} \delta_\mu^m, \quad \omega_\mu^{mn} = -\Omega^{-1} \left(\delta_\mu^m \partial^n \Omega - \delta_\mu^n \partial^m \Omega \right), \quad (2.19)$$

and the above kinetic term becomes

$$S_f = i \int d^4x \left(\frac{1}{\Omega^3} \bar{\Psi} \not{\partial} \Psi + \frac{3}{\Omega^4} \bar{\Psi} (\not{\partial} \Omega) \Psi \right). \quad (2.20)$$

This shows that the fermion sector also receives corrections from nonminimal coupling ξ through the Weyl factor Ω . When expanded in terms of M_{Pl}^{-1} , these corrections correspond to higher dimensional operators. At the $\mathcal{O}(M_{\text{Pl}}^{-2})$, the coefficients of these operators could

have linear ξ -dependence at most. Hence, in the large ξ regime, such corrections from the fermion sector are relatively small as compared with those in the gauge sector.

In summary, we discuss in this section the formulation of the SM coupled to gravity through both minimal and nonminimal couplings in the electroweak vacuum. We derive the relevant Lagrangians and Feynman rules in terms of canonically normalized fields for both Jordan and Einstein frames, which are shown in Appendix A. For the leading order ξ corrections, the graviton contributions are important in Jordan frame, while in Einstein frame it is the effective higher dimensional interactions that are really relevant. From these analyses, we see the advantage of Einstein frame, in which the complicated graviton contributions are transformed away and result in the higher dimensional effective Higgs operators. The latter makes the ξ -induced modifications to the SM sector transparent, and allow us to perform the calculations in a much easier manner.

3 Weak Boson Scattering in Jordan and Einstein Frames

The action (1.5) retains the leading terms in the low energy effective theory that combines the SM and GR. They are perturbatively non-renormalizable in the conventional sense. In both Jordan and Einstein frames, this fact will certainly manifest through the ξ -dependent effective operators with Higgs doublets. In consequence, we observe that for the high energy scattering of longitudinal weak bosons, the scattering amplitudes will generally exhibit non-canceled E^2 behaviors (with E the scattering energy). For $|\xi| \gg 1$, the non-canceled E^2 terms induced by the nonminimal coupling ξ will dominate the amplitudes, and lead to violation of perturbative unitarity. Based on the longitudinal-Goldstone boson equivalence theorem (ET) [16], we expect that the same non-canceled E^2 behavior can be derived from the corresponding Goldstone boson scattering amplitudes. In this section, we will systematically analyze the weak boson scattering with nonzero ξ and demonstrate the ET in both Jordan and Einstein frames. Such demonstrations are highly nontrivial. In Einstein frame, we note that the ξ -dependent scalar derivative interactions (2.16) take very different forms from the new Higgs-gauge boson couplings (2.17). In Jordan frame, we have leading contributions from graviton exchanges. Furthermore, computing the longitudinal and Goldstone amplitudes in both frames will help to demonstrate the equivalence between the two frames, and serve as valuable consistency checks for our analyses.

Then, we derive the perturbative unitarity bound on the nonminimal coupling via coupled channel analysis. For this, we will study all neutral channels of weak bosons and Higgs boson scattering with normalized initial/final states, $|W_L^+ W_L^- \rangle$, $\frac{1}{\sqrt{2}}|Z_L^0 Z_L^0 \rangle$, $\frac{1}{\sqrt{2}}|\phi\phi \rangle$, and $|Z_L^0 \phi \rangle$, as well as the corresponding Goldstone boson processes with initial/final states

$|\pi^+\pi^-\rangle$, $\frac{1}{\sqrt{2}}|\pi^0\pi^0\rangle$, $\frac{1}{\sqrt{2}}|\phi\phi\rangle$, and $|\pi^0\phi\rangle$. As we will show, the $2 \rightarrow 2$ process involving four identical external particles has vanishing E^2 term from non-minimal coupling, due to the crossing symmetry among (s, t, u) channels. The rest of non-trivial processes can be classified into two categories, depending on whether the in/out states contain Higgs boson or not. The amplitudes in each category have similar form. In the following, we will investigate these two types of processes for the weak boson and Goldstone boson scatterings in each frame. We explicitly demonstrate the ET in both frames and show the equivalence of computations between the two frames. Finally, we will derive the perturbative unitarity bound on the Higgs-gravity coupling ξ and analyze the probe of ξ -induced weak boson scatterings at the LHC (14 TeV) and the future high energy pp colliders (50 – 100 TeV) [25]. These also systematically extend our recent short study [15] (which was for the Einstein frame alone and only to the first order of $1/M_{\text{Pl}}^2$).

3.1 Analysis in Jordan Frame

We start our analysis in Jordan frame. The first category of processes is for the weak boson scatterings, with initial/final states containing no Higgs boson ϕ . For demonstration, we first consider the sample process $W_L^+W_L^- \rightarrow Z_L^0Z_L^0$. There are four SM-types of Feynman diagrams contributing to this process at tree-level, as shown in Fig. 1, except that the invoked Higgs-gauge-boson couplings are modified from the corresponding SM couplings. We present the relevant Feynman rules in Appendix A.1.

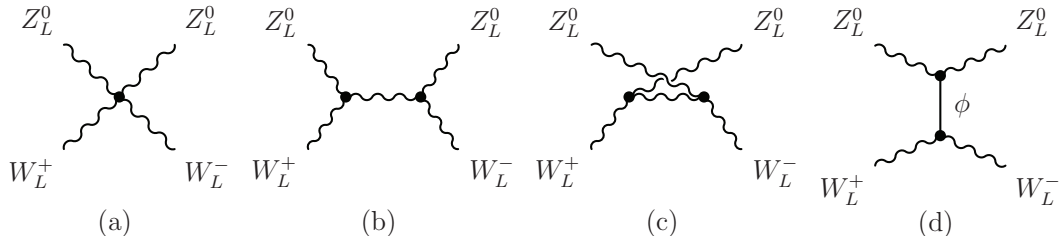


Figure 1. Weak boson scattering process $W_L^+W_L^- \rightarrow Z_L^0Z_L^0$ at tree-level, via SM-type diagrams. The nonminimal coupling ξ leads to anomalous Higgs-gauge-boson couplings in (d).

While the pure gauge couplings remain unchanged in Jordan frame, there are two new ingredients in Higgs couplings. One is the Higgs rescaling factor ζ [cf. (2.4)-(2.5)] for each vertex with Higgs field(s), and the other is the Higgs component in the original perturbed metric $\hat{h}_{\mu\nu}$ [cf. (2.4),(2.9)]. The former causes $\mathcal{O}(\xi^2/M_{\text{Pl}}^2)$ corrections to the SM Higgs coupling, while the latter induces a new Higgs coupling of $\mathcal{O}(\xi/M_{\text{Pl}}^2)$ to the trace of stress tensor of gauge bosons. With these, we compute the diagram with s -channel Higgs exchange

in Fig. 1(d),

$$\mathcal{T}_\phi^s(W_L^+W_L^- \rightarrow Z_L^0Z_L^0) = -\left(1 - \frac{\xi v^2}{M_{\text{Pl}}^2}\right)^2 \frac{\zeta^2 E^4}{v^2(E^2 - m_\phi^2)}, \quad (3.1)$$

where E is the center-of-mass energy. At $\mathcal{O}(E^2)$, the other three pure gauge-boson diagrams in Fig. 1 contribute to the amplitude with $\mathcal{O}(E^2/v^2)$ terms. Thus, we deduce the full amplitude to all orders in ξ^2/M_{Pl}^2 ,

$$\begin{aligned} \mathcal{T}(W_L^+W_L^- \rightarrow Z_L^0Z_L^0) &= \left[1 - \left(1 - \frac{\xi v^2}{M_{\text{Pl}}^2}\right)^2 \zeta^2\right] \frac{E^2}{v^2} + \mathcal{O}(E^0) \\ &= \left[\frac{6\xi^2 + 2\xi}{M_{\text{Pl}}^2} - \frac{36\xi^4 v^2}{M_{\text{Pl}}^4}\right] E^2 + \mathcal{O}(E^0, M_{\text{Pl}}^{-6}), \end{aligned} \quad (3.2)$$

where in the second step we have expanded the amplitude up to $\mathcal{O}(\xi^4/M_{\text{Pl}}^4)$ for comparison. We have also kept the first subleading term of $\mathcal{O}(\xi/M_{\text{Pl}}^2)$ at the lowest order in $1/M_{\text{Pl}}^2$ expansion. As will be clear later, for $|\xi| \gg \mathcal{O}(1)$, the amplitudes are dominated by the leading terms with the form of $(\xi/M_{\text{Pl}})^{2n}$.

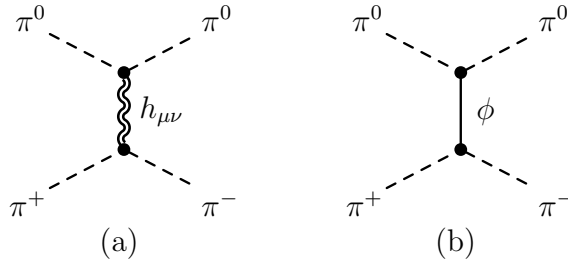


Figure 2. Goldstone boson scattering process $\pi^+\pi^- \rightarrow \pi^0\pi^0$ in Jordan frame, via the s -channel graviton exchange in plot-(a), and the s -channel Higgs boson exchange in plot-(b).

Next, we compute the amplitude of the corresponding Goldstone boson scattering $\pi^+\pi^- \rightarrow \pi^0\pi^0$. At the order of E^2/M_{Pl}^2 , the only relevant Feynman diagram comes from the s -channel graviton exchange, as shown in Fig. 2(a). Thus, we deduce

$$\mathcal{T}_h^s(\pi^+\pi^- \rightarrow \pi^0\pi^0) = \left[(6\xi^2 + 2\xi) + \frac{1 - \cos^2\theta}{4}\right] \frac{E^2}{M_{\text{Pl}}^2} + \mathcal{O}(E^0), \quad (3.3)$$

where θ is the scattering angle. Eq. (3.3) is dominated by the ξ -dependent contributions for $|\xi| \gg 1$. There is no correction of $\mathcal{O}(1/M_{\text{Pl}}^4)$ or higher to this tree-level process. On the other hand, for the diagram with the s -channel Higgs exchange in Fig. 2(b), its contribution to the E^2 -amplitude starts only at the order of M_{Pl}^{-4} . At each order in M_{Pl}^{-1} , we only consider leading ξ -terms of the form $(\xi/M_{\text{Pl}})^{2n}$, except that at the lowest order of M_{Pl}^{-2} , we retain the subleading term of $\mathcal{O}(\xi/M_{\text{Pl}}^2)$. It is clear that the leading terms of $(\xi/M_{\text{Pl}})^{2n}$

always dominate the amplitudes for $|\xi| \gg 1$. We note that such leading terms arise from the ξ -enhanced effective operators and the rescaling factor ζ (cf. Sec. 2). Thus, we infer the following expression for Fig. 2(b), at the $\mathcal{O}(E^2)$ and to all orders in (ξ/M_{Pl}) ,

$$\mathcal{T}_\phi^s(\pi^+\pi^-\rightarrow\pi^0\pi^0) = -\frac{36\zeta^2\xi^4v^2}{M_{\text{Pl}}^4}E^2 + \mathcal{O}(E^0). \quad (3.4)$$

Thus, summing up (3.3) and (3.4), we have the full Goldstone amplitude at $\mathcal{O}(E^2)$,

$$\mathcal{T}(\pi^+\pi^-\rightarrow\pi^0\pi^0) = \mathcal{T}_h^s + \mathcal{T}_\phi^s = \left[\frac{6\xi^2 + 2\xi}{M_{\text{Pl}}^2} - \frac{36\xi^4v^2}{M_{\text{Pl}}^4} \right] E^2 + \mathcal{O}(E^0), \quad (3.5)$$

where we only keep ξ -dependent terms which dominate the amplitude for $|\xi| \gg 1$. The Goldstone amplitude (3.5) agrees well with that of the longitudinal scattering in Eq. (3.2). Hence, this explicitly demonstrates the longitudinal-Goldstone boson equivalence theorem with nonminimal coupling ξ in the Jordan frame.

The second type of processes involves at least a pair of Higgs bosons in the external states. For illustration, we consider the scattering $W_L^+W_L^- \rightarrow \phi\phi$. In unitary gauge, the tree-level contributions to this process are shown in Fig. 3. We see that graviton also plays a role, because its coupling with the Higgs boson ϕ receives large ξ -enhancement directly from the nonminimal coupling term.

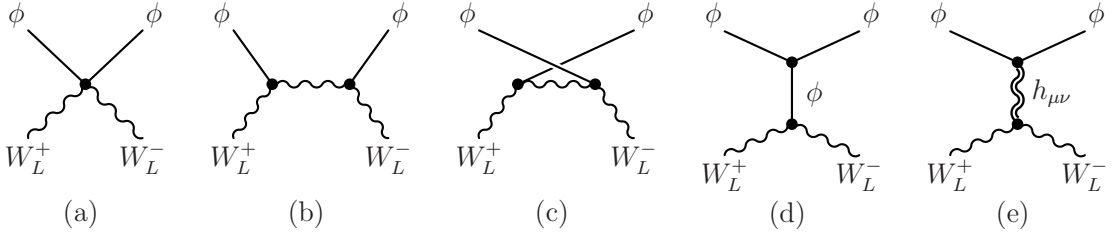


Figure 3. Longitudinal weak boson scattering process $W_L^+W_L^- \rightarrow \phi\phi$ in the presence of nonminimal coupling ξ , where the last diagram arises from the graviton exchange in Jordan frame.

Using the Feynman rules of Appendix A.1, we evaluate the relevant diagrams in Fig. 3,

$$\text{Fig. 3(a)} = \left(1 - \frac{4\xi v^2}{M_{\text{Pl}}^2}\right) \zeta^2 \frac{E^2}{v^2} + \mathcal{O}(E^0), \quad (3.6a)$$

$$\text{Fig. 3(b)+(c)} = -\left(1 - \frac{2\xi v^2}{M_{\text{Pl}}^2}\right) \zeta^2 \frac{E^2}{v^2} + \mathcal{O}(E^0), \quad (3.6b)$$

$$\text{Fig. 3(d)} = -\frac{6\xi^2 - \xi}{M_{\text{Pl}}^2} \zeta^4 E^2 + \mathcal{O}(E^0), \quad (3.6c)$$

$$\text{Fig. 3(e)} = -\frac{\xi + \mathcal{O}(\xi^0)}{M_{\text{Pl}}^2} \zeta^2 E^2 + \mathcal{O}(E^0). \quad (3.6d)$$

Summing up all these diagrams, we deduce the scattering amplitude at $\mathcal{O}(E^2)$, including all leading terms of $(\xi/M_{\text{Pl}})^{2n}$,

$$\begin{aligned}\mathcal{T}(W_L^+ W_L^- \rightarrow \phi\phi) &= -\zeta^2 \left[1 + \frac{3\xi v^2}{M_{\text{Pl}}^2} - \left(1 + \frac{\xi v^2}{M_{\text{Pl}}^2} \right) \zeta^2 \right] \frac{E^2}{v^2} + \mathcal{O}(E^0) \\ &= - \left[\frac{6\xi^2 + 2\xi}{M_{\text{Pl}}^2} - \frac{72\xi^4 v^2}{M_{\text{Pl}}^4} \right] E^2 + \mathcal{O}(E^0, M_{\text{Pl}}^{-6}),\end{aligned}\tag{3.7}$$

where we have also retained the first subleading term of $\mathcal{O}(\xi/M_{\text{Pl}}^2)$ as before.

It is interesting to note that the above amplitude (3.7) coincides with that of $W_L^+ W_L^- \rightarrow Z_L^0 Z_L^0$ in (3.2) at the leading order of M_{Pl}^{-2} , except to an overall minus sign. This becomes more transparent when we check the corresponding Goldstone scattering amplitude of $\pi^+ \pi^- \rightarrow \phi\phi$. Similar to $\pi^+ \pi^- \rightarrow \pi^0 \pi^0$, only the diagram with s -channel graviton exchange contributes at $\mathcal{O}(E^2/M_{\text{Pl}}^2)$, with the final state $\pi^0 \pi^0$ replaced by $\phi\phi$ in Fig. 2. Applying the Feynman rules of Appendix A.1, we compute the leading amplitude at $\mathcal{O}(M_{\text{Pl}}^{-2})$,

$$\mathcal{T}(\pi^+ \pi^- \rightarrow \phi\phi) = \frac{6\xi^2 + 2\xi + \mathcal{O}(\xi^0)}{M_{\text{Pl}}^2} E^2 + \mathcal{O}(E^0, M_{\text{Pl}}^{-4}),\tag{3.8}$$

which coincides with (3.3) due to the universal coupling of graviton at leading order of M_{Pl}^{-2} . According to the equivalence theorem [16],

$$\mathcal{T}(W_L^{a_1}, \dots, W_L^{a_n}, X) = \mathcal{T}(-i\pi^{a_1}, \dots, -i\pi^{a_n}, X) + \mathcal{O}(m_W/E_j \text{ suppressed}),\tag{3.9}$$

where X represents other physical on-shell states. Hence, for the $2 \rightarrow 2$ scattering, a difference of overall minus sign between (3.7) and (3.8) is expected, due to the factor $(-i)^2 = -1$ associated with the two external Goldstone fields $\pi^+ \pi^-$ on the right-hand-side of (3.9).

For all other processes, we find full agreement between the longitudinal scattering amplitudes and the corresponding Goldstone scattering amplitudes by explicit calculations, for $E^2 \gg m_W^2$. This justifies the longitudinal-Goldstone boson equivalence theorem in the presence of Higgs-gravity interactions with nonzero ξ coupling. In the following, we summarize all the $\mathcal{O}(E^2)$ Goldstone amplitudes for the electrically neutral channels, which include all leading terms of $(\xi/M_{\text{Pl}})^{2n}$. We will also retain the first subleading term of $\mathcal{O}(\xi/M_{\text{Pl}}^2)$. Thus, we arrive at,

$$\begin{aligned}\mathcal{T}(\pi^+ \pi^- \rightarrow \pi^+ \pi^-) &= \left[1 - \left(1 - \frac{2\xi v^2}{M_{\text{Pl}}^2} \right) \zeta^2 \right] \frac{(1 + \cos \theta)}{2v^2} E^2 \\ &\simeq \left[\frac{3\xi^2 + \xi}{M_{\text{Pl}}^2} - \frac{18\xi^4 v^2}{M_{\text{Pl}}^4} \right] (1 + \cos \theta) E^2,\end{aligned}\tag{3.10a}$$

$$\mathcal{T}(\pi^+ \pi^- \rightarrow \pi^0 \pi^0) = \left[1 - \left(1 - \frac{2\xi v^2}{M_{\text{Pl}}^2} \right) \zeta^2 \right] \frac{E^2}{v^2}$$

$$\simeq \left[\frac{6\xi^2 + 2\xi}{M_{\text{Pl}}^2} - \frac{36\xi^4 v^2}{M_{\text{Pl}}^4} \right] E^2, \quad (3.10b)$$

$$\mathcal{T}(\pi^0 \pi^0 \rightarrow \pi^0 \pi^0) = \mathcal{O}(E^0), \quad (3.10c)$$

$$\begin{aligned} \mathcal{T}(\pi^+ \pi^- \rightarrow \phi\phi) &= \left[1 + \frac{3\xi v^2}{M_{\text{Pl}}^2} - \left(1 + \frac{\xi v^2}{M_{\text{Pl}}^2} \right) \zeta^2 \right] \zeta^2 \frac{E^2}{v^2} \\ &\simeq \left[\frac{6\xi^2 + 2\xi}{M_{\text{Pl}}^2} - \frac{72\xi^4 v^2}{M_{\text{Pl}}^4} \right] E^2, \end{aligned} \quad (3.10d)$$

$$\begin{aligned} \mathcal{T}(\pi^0 \pi^0 \rightarrow \phi\phi) &= \left[1 + \frac{3\xi v^2}{M_{\text{Pl}}^2} - \left(1 + \frac{\xi v^2}{M_{\text{Pl}}^2} \right) \zeta^2 \right] \zeta^2 \frac{E^2}{v^2} \\ &\simeq \left[\frac{6\xi^2 + 2\xi}{M_{\text{Pl}}^2} - \frac{72\xi^4 v^2}{M_{\text{Pl}}^4} \right] E^2, \end{aligned} \quad (3.10e)$$

$$\begin{aligned} \mathcal{T}(\pi^0 \phi \rightarrow \pi^0 \phi) &= - \left[1 + \frac{3\xi v^2}{M_{\text{Pl}}^2} - \left(1 + \frac{\xi v^2}{M_{\text{Pl}}^2} \right) \zeta^2 \right] \frac{(1 - \cos \theta)}{2v^2} \zeta^2 E^2 \\ &\simeq - \left[\frac{3\xi^2 + \xi}{M_{\text{Pl}}^2} - \frac{36\xi^4 v^2}{M_{\text{Pl}}^4} \right] (1 - \cos \theta) E^2, \end{aligned} \quad (3.10f)$$

$$\mathcal{T}(\phi\phi \rightarrow \phi\phi) = \mathcal{O}(E^0). \quad (3.10g)$$

These serve as highly nontrivial self-consistency checks of the scattering amplitudes in Jordan frame. The above can be compared with our previous results in Einstein frame [15], which were computed at $\mathcal{O}(M_{\text{Pl}}^{-2})$ only. Also, we note that Ref. [26] studied linearized gravity in the presence of a nonminimal coupling term $\xi R\phi^2$ (with singlet scalar ϕ) in Jordan frame. They calculated scattering amplitudes for external spin-(0, 1/2, 1) particles from graviton-exchange at $\mathcal{O}(M_{\text{Pl}}^{-2})$, where the singlet scalar ϕ has no VEV. From our results in (3.10) with the SM Higgs doublet, we find that the leading ξ contributions at $\mathcal{O}(M_{\text{Pl}}^{-2})$ do not depend on the Higgs VEV. Thus, for the singlet scalar scattering process like $ss \rightarrow s's'$, our result reduces to that of Ref. [26] at $\mathcal{O}(M_{\text{Pl}}^{-2})$.

3.2 Analysis in Einstein Frame

In this subsection, we proceed with the analysis in Einstein frame. To demonstrate the nontrivial difference of the current analysis from that in Jordan frame, we will present explicit calculations for the two processes considered in the previous subsection.

We first compute the amplitude of $W_L^+ W_L^- \rightarrow Z_L^0 Z_L^0$ with the Lagrangian (2.17). In unitary gauge, the contribution to the scattering amplitudes with positive power of scattering energy E comes from the same diagrams as in Jordan frame in Fig. 1. As shown in Appendix A, the ξ corrections to the cubic Higgs-gauge-boson couplings are the same in both frames. Hence, the amplitude from Fig. 1(d) remains intact, and the sum of the four

diagrams should equal that of (3.2) in the Jordan frame. In parallel, we consider the corresponding Goldstone boson scattering process $\pi^+\pi^-\rightarrow\pi^0\pi^0$. Here, the deviation from the SM is from higher dimensional operators in the Lagrangian (2.16). Using the Feynman rules in Appendix A.2, we find that the leading amplitude for this process arises from the contact interaction,

$$\mathcal{T}(\pi^+\pi^-\rightarrow\pi^0\pi^0)=\left[\frac{6\xi^2+2\xi}{M_{\text{Pl}}^2}-\frac{36\xi^4v^2}{M_{\text{Pl}}^4}\right]E^2+\mathcal{O}(E^0,M_{\text{Pl}}^{-6}),\quad(3.11)$$

which coincides with the amplitude of $W_L^+W_L^-\rightarrow Z_L^0Z_L^0$. This shows that the longitudinal-Goldstone boson equivalence theorem holds for this process in Einstein frame, and the derived scattering amplitudes in both frames are consistent. For the sake of later physical analysis, we present the amplitudes of $W_L^\pm W_L^\pm\rightarrow W_L^\pm W_L^\pm$ and $\pi^\pm\pi^\pm\rightarrow\pi^\pm\pi^\pm$ as well. By crossing symmetry, we infer from (3.11),

$$\begin{aligned}\mathcal{T}(W_L^\pm W_L^\pm\rightarrow W_L^\pm W_L^\pm)&\simeq\mathcal{T}(\pi^\pm\pi^\pm\rightarrow\pi^\pm\pi^\pm) \\ &=-\left[\frac{6\xi^2+2\xi}{M_{\text{Pl}}^2}-\frac{36\xi^4v^2}{M_{\text{Pl}}^4}\right]E^2+\mathcal{O}(E^0,M_{\text{Pl}}^{-6}).\end{aligned}\quad(3.12)$$

Next, we analyze the other scattering process $W_L^+W_L^-\rightarrow\phi\phi$. Different from the case in Jordan frame, no ξ -contribution arises from the graviton-exchange diagram in Fig. 3(e). Hence, only the first four diagrams of Fig. 3 are relevant to our study in Einstein frame. With the Feynman rules of Appendix A.2, we find a difference for the diagram of Fig. 3(a) between the two frames, while the diagrams (b), (c) and (d) remain intact. Despite such a difference, we have verified the following equality at $\mathcal{O}(E^2)$,

$$[\text{Fig. 3(a)}+\text{Fig. 3(e)}]_{\text{Jordan}}=\text{Fig. 3(a)}_{\text{Einstein}}.\quad(3.13)$$

Hence, the amplitude fully coincides with that in the Jordan frame. This explicitly demonstrates the equivalence between the two frames via the above scattering process. For the corresponding Goldstone boson scattering, it receives contributions from contact interaction as well as s -channel Higgs exchange. We find the same result as (3.8) at the leading order.

Then, we systematically extend the above calculations to all other scattering channels. We reveal that for both the longitudinal gauge boson scattering and Goldstone boson scattering, the results coincide with those in the Jordan frame. As an advantage of the Einstein frame analysis, it is easier to extract the ξ -dependent E^2 -terms without invoking tedious calculations with the graviton-exchange. Here we present the amplitudes at $\mathcal{O}(E^2)$, keeping all the leading power terms of $(\xi/M_{\text{Pl}})^n$, but dropping the subleading terms in which the power of ξ is lower than that of $(\xi/M_{\text{Pl}})^n$ at each given order of $1/M_{\text{Pl}}^n$. We find that so

long as $\xi > \mathcal{O}(1)$, this always gives a good approximation for our unitarity analysis in the next subsection.

$$\begin{aligned}
\mathcal{T}(\pi^+\pi^- \rightarrow \pi^+\pi^-) &= \frac{(1-\zeta^2)}{2v^2}(1+\cos\theta)E^2, \\
\mathcal{T}(\pi^+\pi^- \rightarrow \pi^0\pi^0) &= \frac{(1-\zeta^2)}{v^2}E^2, \\
\mathcal{T}(\pi^0\pi^0 \rightarrow \pi^0\pi^0) &= \mathcal{O}(E^0), \\
\mathcal{T}(\pi^+\pi^- \rightarrow \phi\phi) &= \frac{(1-\zeta^2)\zeta^2}{v^2}E^2, \\
\mathcal{T}(\pi^0\pi^0 \rightarrow \phi\phi) &= \frac{(1-\zeta^2)\zeta^2}{v^2}E^2, \\
\mathcal{T}(\pi^0\phi \rightarrow \pi^0\phi) &= -\frac{(1-\zeta^2)\zeta^2}{2v^2}(1-\cos\theta)E^2, \\
\mathcal{T}(\phi\phi \rightarrow \phi\phi) &= \mathcal{O}(E^0).
\end{aligned} \tag{3.14}$$

We note that the $(\xi/M_{\text{Pl}})^n$ terms originate from the ξ -enhanced effective operators and the rescaling factor ζ . As a consistency check, we note that the above expressions reduce to (3.10) at $\mathcal{O}(\xi^2/M_{\text{Pl}}^2)$ and $\mathcal{O}(\xi^4/M_{\text{Pl}}^4)$ under the $1/M_{\text{Pl}}$ expansion.

So far, as a by product, we have explicitly demonstrated the equivalence between Jordan frame and Einstein frame for high energy scattering of weak bosons and Higgs bosons under the flat background metric. There are debates on the physical (in)equivalence between Jordan and Einstein frames in the literature [10, 11, 17–19]. Our study supports the equivalence of the two frames from the tree-level analysis of weak boson and Higgs boson scatterings (which were not considered before). The reason is that we can take the spacetime be flat in both frames, and then the frame transformation is just a nonlinear field redefinition. According to the theorem á la CCWZ [27], a field redefinition $\phi \rightarrow f(\phi)$ will not change the on-shell S -matrix involving ϕ , provided that the nonlinear local transformation $f(\phi)$ has the form $f(\phi) = \phi F(\phi)$ where $F(\phi)$ is another local function of ϕ satisfying $F(0) = 1$. This is exactly the case for the canonical degrees of freedom in the two frames, as we explicitly demonstrated in (2.14). Hence, we should expect the same results for high energy weak boson scatterings in both frames.

In passing, we note that the equivalence of the two frames is more involved beyond tree-level, as pointed out before [8, 10, 11, 18, 19]. Due to the quantum anomaly from the Weyl transformation between the two frames and the unknown UV dynamics of quantum gravity, the loop analysis and renormalization prescriptions would suffer ambiguity. For example, there are different ways of choosing renormalization scale μ , concerning whether μ is field-

independent in Einstein frame or in Jordan frame [18]. A possible prescription of realizing the frame-equivalence at quantum level was recently discussed in [19].

Before concluding this section, we make further remarks on the physical impact of the leading order ξ corrections to the scattering amplitudes (3.10). At the first nontrivial order of M_{Pl}^{-2} , we have both ξ^2 and ξ contributions to the amplitudes, where the ξ^2 terms are dominant for $|\xi| \gg 1$. Its impact can be classified into three categories. The first one is a universal suppression factor $\zeta < 1$ for any coupling involving the Higgs field, such as the Higgs boson production process [14]. The second class of ξ^2 -dependent processes are the weak boson scatterings which we study in this paper. We have analyzed the *anomalous* cubic Higgs-gauge coupling and quartic scalar couplings in Einstein frame, and computed the graviton-exchanges in Jordan frame. We find that they cause non-canceled ξ^2 (and ξ) dependent E^2 -contributions in the longitudinal and Goldstone boson scattering amplitudes, which can become significant as the increase of scattering energy E . Hence, the longitudinal WW scattering can provide sensitive probe of ξ coupling via energy-enhanced leading contributions of $\mathcal{O}(\xi^2 E^2/M_{\text{Pl}}^2)$. The third class of ξ^2 -involved processes are those containing the cubic Higgs self-coupling. As shown in (2.16), such processes will also be enhanced at high energies by the ξ^2 -dependent derivative cubic Higgs couplings. The future high energy pp colliders (50 – 100 TeV) [25] will further probe such anomalous cubic Higgs couplings. Finally, the $\mathcal{O}(\xi/M_{\text{Pl}}^2)$ terms arise from the Weyl factor Ω , including bosonic and fermionic couplings of the Higgs boson. But they are negligible relative to the leading contributions of $\mathcal{O}(\xi^2/M_{\text{Pl}}^2)$ for $|\xi| \gg 1$.

3.3 Perturbative Unitarity Bound on Higgs-Gravity Coupling

In the above two subsections, we have derived the high energy weak boson scattering amplitudes in the Jordan and Einstein frames, and demonstrated the longitudinal-Goldstone boson equivalence theorem in both frames. We further showed that the two frames give the same scattering amplitudes. With these, we will derive perturbative unitarity bound on the Higgs-gravity coupling ξ via coupled channel analysis in this subsection.

Given the scattering amplitudes in the previous subsections, we compute the partial wave amplitudes for the Goldstone and Higgs bosons,

$$a_\ell(E) = \frac{1}{32\pi} \int_{-1}^1 d\cos\theta P_\ell(\cos\theta) \mathcal{T}(E, \theta). \quad (3.15)$$

For the present case, the partial wave amplitudes form a 4×4 matrix among the four initial/final states, $|\pi^+\pi^-\rangle$, $\frac{1}{\sqrt{2}}|\pi^0\pi^0\rangle$, $\frac{1}{\sqrt{2}}|h^0h^0\rangle$, and $|\pi^0h^0\rangle$. In coupled channel analysis, we will impose the s -wave unitarity condition, $|\Re a_0| < 1/2$, on the maximal eigenvalue of the matrix a_0 .

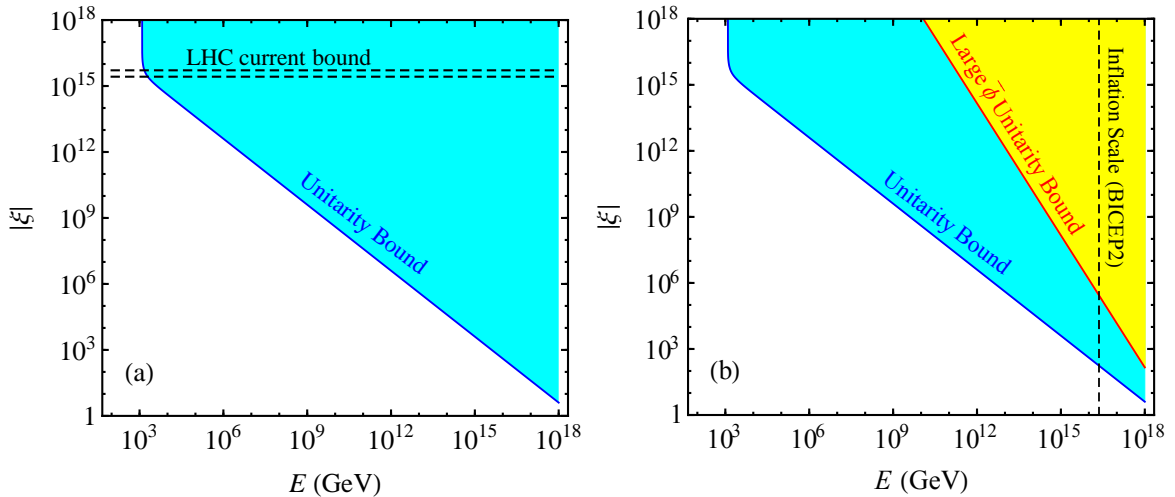


Figure 4. Perturbative unitarity bound on the Higgs-gravity coupling ξ as a function of center-of-mass energy E . In plot-(a), the blue curve denotes the bound derived at $\bar{\phi} = v$, where the shaded region violates perturbative unitarity. In plot-(b), we further present the unitarity bound at large background field $\bar{\phi} = M_{\text{Pl}}/\sqrt{\xi}$ (red curve), as compared to the unitarity bound at $\bar{\phi} = v$ (blue curve). The shaded yellow area above the red curve violates perturbative unitarity, and its physical implications will be explained in Sec. 4.3. The vertical dashed line denotes the inflation scale (2.3×10^{16} GeV) as indicated by the BICEP2 data [24]. For comparison, the upper (lower) horizontal dashed line in plot-(a) denotes the 3σ bound $|\xi| < 5.2 \times 10^{15}$ ($|\xi| < 2.7 \times 10^{15}$) derived from the current CMS (ATLAS) Higgs data [2] at the LHC.

From (3.14), we deduce the following s -wave amplitude at $\mathcal{O}(E^2)$ and to all orders in (ξ/M_{Pl}) ,

$$a_0(E) = \frac{(1 - \zeta^2)E^2}{32\pi v^2} \begin{pmatrix} 1 & \sqrt{2} & \sqrt{2}\zeta^2 & 0 \\ \sqrt{2} & 0 & \zeta^2 & 0 \\ \sqrt{2}\zeta^2 & \zeta^2 & 0 & 0 \\ 0 & 0 & 0 & -\zeta^2 \end{pmatrix}. \quad (3.16)$$

Thus, we further derive its eigenvalues,

$$a_0^{\text{diag}}(E) = \frac{(1 - \zeta^2)E^2}{32\pi v^2} \text{diag}\left(1 + \sqrt{1 + 3\zeta^4}, 1 - \sqrt{1 + 3\zeta^4}, -\zeta^2, -1\right). \quad (3.17)$$

Imposing the partial wave unitarity condition on the maximal eigenvalue of (3.17), we deduce the following perturbative unitarity bound on the scattering energy E for a given value of the ξ coupling,

$$E < \frac{\sqrt{16\pi} v}{\left[(1 - \zeta^2)(1 + \sqrt{1 + 3\zeta^4})\right]^{1/2}}. \quad (3.18)$$

We can translate this into a constraint on the Higgs-curvature coupling ξ at a given energy scale E ,

$$(1 - \zeta^2)(1 + \sqrt{1 + 3\zeta^4}) < \frac{16\pi v^2}{E^2}. \quad (3.19)$$

For most of the parameter range of physical interest, we find that the expansion of ζ in terms of $\xi v/M_{\text{Pl}}$ gives a good approximation. Thus, from (3.19) or (3.18), we may derive a simplified perturbative unitarity bound on the ξ coupling,

$$|\xi| < \frac{\sqrt{8\pi}M_{\text{Pl}}}{3E} \left[1 + \frac{4\pi v^2}{E^2} + \mathcal{O}\left(\frac{v}{E}\right)^4 \right]. \quad (3.20)$$

We see that the expansion in the brackets of the right-hand-side of (3.20) is practically in terms of the ratio v^2/E^2 . Hence, the approximate formula (3.20) works well so long as $E > \mathcal{O}(1\text{TeV})$. We also note that the tree-level unitarity violation is a signal of requiring higher order nonperturbative effects and the inclusion of new resonance(s) in the effective field theory. As we clarified before [15], the perturbative unitarity bounds [28–30] are fully justified and important. Especially, the unitarity bound on the SM Higgs boson mass $m_h < \sqrt{8\pi/3}v \simeq 712\text{ GeV}$ [30] has been well supported by the recent LHC Higgs discovery [1, 2] with $m_h \simeq 125\text{ GeV} (< 712\text{ GeV})$.

In Fig. 4(a), we present the perturbative unitarity bound of ξ as a function of scattering energy E , up to $E = 10^{18}\text{ GeV} \lesssim M_{\text{Pl}}$, by the thick blue curve, where we set $\bar{\phi} = v$ for the electroweak vacuum. It is useful to check a special limit of $\xi \rightarrow \infty$ for the condition (3.19). In this case, we have $\zeta \rightarrow 0$ and the Higgs field decouples. Thus, the bound (3.19) reduces to $E < \sqrt{8\pi}v \simeq 1.23\text{ TeV}$. This bound is nicely reflected by the asymptotical behavior of the blue curve around $E = \mathcal{O}(1\text{TeV})$, as depicted in Fig. 4(a). For the application to Higgs inflations in the next section, we also show the unitarity limit (thick red curve) for the inflation background $\bar{\phi} = M_{\text{Pl}}/\sqrt{\xi}$ in Fig. 4(b), which is significantly relieved than the small field bound at $\bar{\phi} = v$. We will discuss this further in Sec. 4.3.

Fig. 4(a) shows that the unitarity bound puts highly nontrivial constraints on the Higgs-curvature coupling ξ in the perturbative formulation. For the effective theory of the SM + GR with Planck mass M_{Pl} as the UV cutoff, the weak boson scattering energy can reach up to $E = 10^{17-18}\text{ GeV} < M_{\text{Pl}}$. In this case, we find that the perturbative unitarity bound in plot-(a) places stringent new limits, $\xi \lesssim \mathcal{O}(10 - 1)$, for $\bar{\phi} = v$. Besides, we would like to note that Atkins and Calmet [14] derived an interesting bound on ξ from the 2012 LHC data [1]. The latest update of the LHC analyses [2] leads to the Higgs signal strengths, $\hat{\mu} = 1.30 \pm 0.20$ [ATLAS] and $\hat{\mu} = 0.80 \pm 0.14$ [CMS]. From this, we have the refined 3σ upper limits, $|\xi| < 2.7 \times 10^{15}$ [ATLAS] and $|\xi| < 5.2 \times 10^{15}$ [CMS]. For comparison, we

plot the ATLAS and CMS limits in Fig. 4(a) by the horizontal lower and upper dashed lines, respectively. For the electroweak vacuum $\bar{\phi} = v$, we see that once the scattering energy E exceeds $\mathcal{O}(\text{TeV})$, the perturbative unitarity bound becomes much more stringent.

3.4 Probing Higgs-Gravity Coupling via Weak Boson Scattering

It is possible that Nature may have chosen a lower UV cutoff for the effective theory of SM + GR. Thus, the perturbative unitarity bound in Fig. 4 will allow much larger ξ values. An intriguing situation is that the UV cutoff sets in at a scale close to $\mathcal{O}(\text{TeV})$, say, $\Lambda_{\text{UV}} = \mathcal{O}(10\text{TeV})$. Thus, the coupling ξ can reach² $\xi = \mathcal{O}(10^{15})$. Such a relatively low UV cutoff gives a conceptually simple resolution to the hierarchy problem and makes the SM Higgs sector natural up to³ $\Lambda_{\text{UV}} = \mathcal{O}(10\text{TeV})$. This will open up an exciting possibility that the upcoming runs of LHC (14 TeV) and the future high energy pp colliders (50 – 100 TeV) [25] can effectively probe such Higgs-gravity interactions with $\xi = \mathcal{O}(10^{14-15})$ via weak boson scattering experiments.

The weak boson scattering is a crucial experiment for the LHC to test new physics of electroweak symmetry breaking beyond the SM Higgs sector [31]. Hence, we study the weak boson scattering cross sections, and analyze three major processes, $W_L^+ W_L^- \rightarrow Z_L^0 Z_L^0$, $W_L^\pm W_L^\pm \rightarrow W_L^\pm W_L^\pm$, and $W_L^\pm Z_L^0 \rightarrow W_L^\pm Z_L^0$. For our study, we consider the intriguing effective theory of low scale quantum gravity with two sample UV cutoffs, $\Lambda_{\text{UV}} = \mathcal{O}(10\text{TeV})$ or $\Lambda_{\text{UV}} = \mathcal{O}(50\text{TeV})$. For tests at the LHC (14 TeV), we consider the effective theory with $\Lambda_{\text{UV}} = \mathcal{O}(10\text{TeV})$. The relevant energy range for the WW scattering at the LHC is around 0.2 – 4 TeV. From Fig. 4(a), we find that for the WW scattering energy $E < 4\text{TeV}$, the size of the Higgs-curvature coupling can be fairly large, $\xi \lesssim \mathcal{O}(10^{15})$. In Fig. 5(a)-(c), we present the WW scattering cross sections for two sample inputs, $\xi = 2 \times 10^{15}, 10^{15}$, in comparison with the SM result of $\xi = 0$. In all three plots (a)-(c), we have input the Higgs boson mass $m_h = 125\text{GeV}$ based on the LHC data [1, 2]. To remove the special kinematical region of t/u -channel diagrams around $\theta = 0, \pi$, we add a modest cut $|\cos\theta| < 0.995$ for all plots. Furthermore, we also place the unitarity condition on the scattering cross section, $\sigma < 4\pi\rho_e/E^2$ [32]. The shaded light-blue region in each plot of Fig. 5 violates perturbative unitarity. (In this condition, ρ_e denotes the identical particle factor for final state of elastic

²From the theory side, we have no preferred natural values for the dimensionless coupling ξ . Note that the ξ coupling in the Feynman vertices is always suppressed by the factor v^2/M_{Pl}^2 or E^2/M_{Pl}^2 [cf. (2.16)-(2.17)]. Hence, a large ξ coupling is fine so long as it respects the perturbation expansion (Fig. 4).

³For the current effective theory study, we are not concerned with any detail of the UV dynamics above $\Lambda_{\text{UV}} = \mathcal{O}(10\text{TeV})$. Many well-motivated TeV scale quantum gravity theories exist on the market. For instance, an extra dimensional model with compactification scale of $\mathcal{O}(10\text{TeV})$ will reveal its Kaluza-Klein modes at energies above this scale.

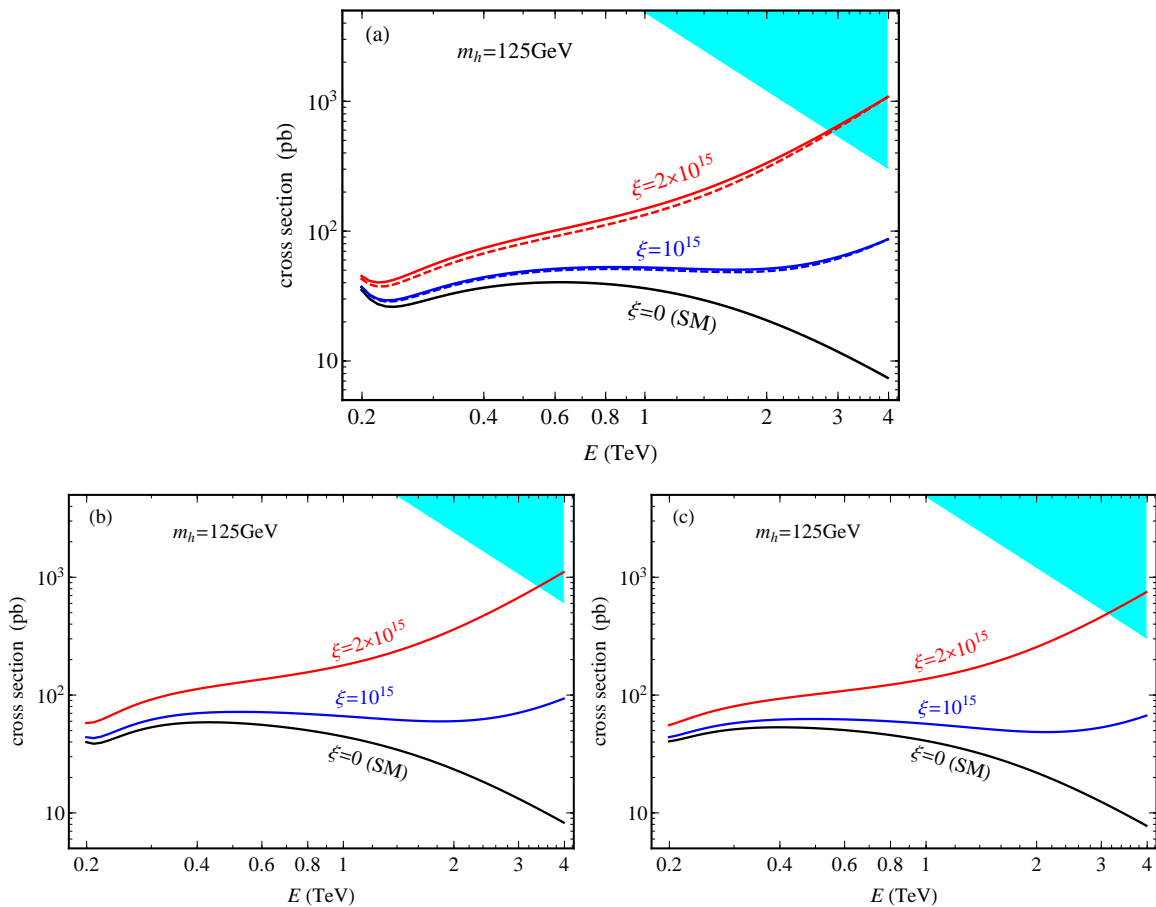


Figure 5. Cross sections of weak boson scattering with Higgs-gravity coupling ξ for the relevant energy range at the LHC (14 TeV). Plot-(a): $W_L^+ W_L^- \rightarrow Z_L^0 Z_L^0$. Plot-(b): $W_L^\pm W_L^\pm \rightarrow W_L^\pm W_L^\pm$. Plot-(c): $W_L^+ Z_L^0 \rightarrow W_L^+ Z_L^0$. In each plot, we depict the predictions for $\xi = (2 \times 10^{15}, 10^{15}, 0)$ by the (red, blue, black) curves. The pure SM result ($\xi = 0$) is given by the black curve. We have input the Higgs boson mass $m_h = 125$ GeV. The shaded (light-blue) region violates perturbative unitarity. The dashed curves in plot-(a) include the RG running of ξ , with initial values taken at $E = 4$ TeV.

channel, and for inelastic channel ρ_e is fixed by the corresponding elastic channel with the same initial state as the inelastic channel [32].)

With the sample inputs $\xi = 10^{15}$ and $\xi = 2 \times 10^{15}$ for Fig. 5(a)-(c), we see that the WW scattering cross sections exhibit different behaviors and give sizable excesses above the SM expectations ($\xi = 0$). We note that these non-resonance behaviors are universal and are predicted to show up in all weak boson scattering channels⁴, in contrast to the traditional new physics models of the electroweak symmetry breaking [31]. The upcoming runs of the LHC (14 TeV) and the upgraded high luminosity LHC will discriminate such

⁴For TeV scale quantum gravity via the spontaneous dimensional reduction approach (with a 125 GeV non-SM Higgs boson), we found universal behaviors of non-resonant WW scattering manifested in a different manner [33]. For a light non-SM Higgs boson in the 4d effective Lagrangian (without gravity), deviations in the non-resonant WW scattering were studied for the LHC before [34].

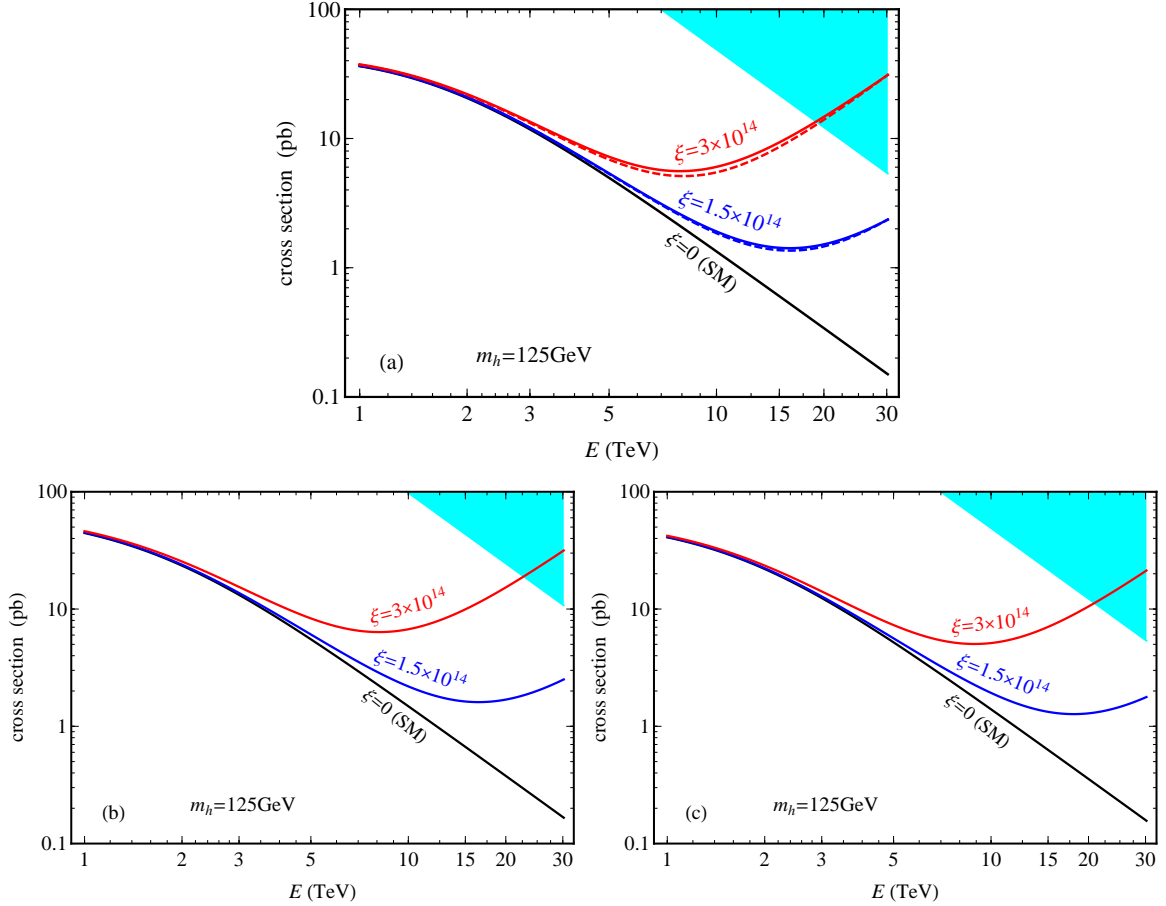


Figure 6. Cross sections of weak boson scattering with Higgs-gravity coupling ξ for the relevant energy range at the future pp collider (50 – 100 TeV). Plot-(a): $W_L^+ W_L^- \rightarrow Z_L^0 Z_L^0$. Plot-(b): $W_L^\pm W_L^\pm \rightarrow W_L^\pm W_L^\pm$. Plot-(c): $W_L^+ Z_L^0 \rightarrow W_L^+ Z_L^0$. In each plot, we depict the predictions for $\xi = (3 \times 10^{14}, 1.5 \times 10^{14}, 0)$ by the (red, blue, black) curves. The pure SM result ($\xi = 0$) is given by the black curve. We have input the Higgs boson mass $m_h = 125$ GeV. The shaded (light-blue) region violates perturbative unitarity. The dashed curves in plot-(a) include the RG running of ξ , with initial values taken at $E = 30$ TeV.

distinctive features of the weak boson scattering signals.

For the present analysis, we have also examined renormalization group (RG) running effects of the ξ coupling. The one-loop RG beta function for ξ is given by [6],

$$\beta(\xi) = \frac{1 + 6\xi}{(4\pi)^2} \left(2\lambda + y_t^2 - \frac{3}{4}g^2 - \frac{1}{4}g'^2 \right), \quad (3.21)$$

where (g, g') are the electroweak gauge couplings, and (λ, y_t) denote the Higg self-coupling and top-quark Yukawa coupling, respectively. The RG equation (3.21) was derived by treating gravity as external field [6]. Using quantized metric and including gravitons in the loop will contribute additional subleading terms of $\mathcal{O}(\xi^0)$, as shown in Ref. [10]. But, for the present study with large values of $\xi \gg 1$, it is safe to use the approximate RG equation (3.21), where the leading ξ -terms fully dominate the coupling running. For numerical analysis of

Eq. (3.21), we take initial values $\xi = 10^{15}$ and 2×10^{15} , respectively, at $E = 4$ TeV, and run the ξ coupling downward with the β function (3.21). We compute the RG improved cross sections by including this running ξ coupling. We plot the RG improved cross sections in Fig. 5(a) as dashed curves. We compare them with the pure tree-level cross sections (in solid curves), and find that the corrections from the RG running of ξ coupling are fairly small for the relevant LHC energy range.

Next, we study the probe of Higgs-gravity coupling ξ at the future pp collider (50 – 100 TeV) [25]. Thus, we consider a sample effective theory with $\Lambda_{\text{UV}} = \mathcal{O}(50 \text{ TeV})$. The relevant WW scattering energies at such a pp collider will be in the range of 0.5 – 30 TeV. In parallel with Fig. 5, we present the WW scattering cross sections Fig. 6 with the scattering energy $E = 0.5 - 30$ TeV, where we input the Higgs-curvature coupling, $\xi = (3 \times 10^{14}, 1.5 \times 10^{14}, 0)$, as depicted by the (red, blue, black) curves, respectively. We have added a simple cut $|\cos\theta| < 0.995$ in each plot to remove the special kinematical region of t/u -channel diagrams around $\theta = 0, \pi$. In Fig. 6(a), we also plot the RG improved cross sections in dashed curves for nonzero ξ , where we input the initial values $\xi = (3 \times 10^{14}, 1.5 \times 10^{14})$ at $E = 30$ TeV and then include the one-loop RG running effects as functions of the WW scattering energy. This shows that the RG effects of ξ are still negligible over the energy range $E \lesssim 30$ TeV for WW scatterings. From Fig. 6, we see that the sensitivity to probing the ξ coupling may be improved by about a factor of 10 as compared to Fig. 5 for the LHC case. This illustrates the importance of increasing the pp collision energy up to 50 – 100 TeV. It is encouraging to further perform detailed Monte Carlo simulations of the full WW scattering processes at the LHC (14 TeV) and the future pp collider (50 – 100 TeV), where the signals/backgrounds from the full processes $pp \rightarrow jjVV$ ($V = W, Z$) with VV decays will be analyzed. This is fully beyond the current scope and will be considered elsewhere.

4 Unitarity Analysis for Higgs Inflation

In this section, we will extend Sec. 3.1-3.3 to the situation with a generically large background field $\bar{\phi}$, and perform the analysis of perturbative unitarity for the Higgs inflation [7]. In Sec. 4.1, we present the background-dependent formulation. Then, in Sec. 4.2 we derive the weak boson scattering amplitudes for a general background field $\bar{\phi}$. Finally, in Sec. 4.3 we quantitatively analyze the background-dependent unitarity constraints on the parameter space of Higgs inflation for both the conventional Higgs inflation [7] and the improved models [21] in light of the recent BICEP2 data [24].

4.1 Background-Dependent Formulation

We start the analysis in Jordan frame, in parallel with Sec. 3.1. Since the background field $\bar{\phi}$ will vary, we need to define the background-dependent Planck mass, $\bar{M}_{\text{Pl}}^2 \equiv M^2 + \xi\bar{\phi}^2$. Expanding the metric tensor $g_{\mu\nu}^{(J)} = \bar{g}_{\mu\nu}^{(J)} + \bar{\kappa}\hat{h}_{\mu\nu}^{(J)}$ with $\bar{\kappa} \equiv \sqrt{2/\bar{M}_{\text{Pl}}}$, we have the following transformations for diagonalizing the kinetic terms,

$$\hat{h}_{\mu\nu}^{(J)} = h_{\mu\nu}^{(J)} - \eta_{\mu\nu}\xi\bar{\kappa}\bar{\zeta}\bar{\phi}^{(J)}, \quad \hat{\phi} = \bar{\zeta}\phi^{(J)}, \quad (4.1)$$

where $h_{\mu\nu}^{(J)}$ and $\phi^{(J)}$ represent canonical fields in Jordan frame. The modified rescaling factor $\bar{\zeta}$ is given by

$$\bar{\zeta} \equiv (1 + 6\xi^2\bar{\phi}^2/\bar{M}_{\text{Pl}}^2)^{-1/2}. \quad (4.2)$$

In Jordan frame, there is no rescaling of Goldstone field π , and we have $\pi^{(J)} = \pi$. Compared with Eqs. (2.4)-(2.5), this amounts to the replacements, $(v, \kappa, \zeta) \rightarrow (\bar{\phi}, \bar{\kappa}, \bar{\zeta})$.

Then, we make transformations from Jordan frame to Einstein frame. The Weyl factor (2.11) can be rewritten as

$$\Omega^2 = \bar{\Omega}^2 \left[1 + \bar{q} \left(\frac{2\hat{\phi}}{\bar{\phi}} + \frac{\hat{\phi}^2 + |\pi|^2}{\bar{\phi}^2} \right) \right], \quad (4.3)$$

with $\bar{\Omega} \equiv \bar{M}_{\text{Pl}}/M_{\text{Pl}}$ and \bar{q} given by

$$\bar{q} \equiv \frac{\xi\bar{\phi}^2}{M_{\text{Pl}}^2\bar{\Omega}^2} = \frac{\xi\bar{\phi}^2}{M_{\text{Pl}}^2}. \quad (4.4)$$

The scalar kinetic terms become,

$$\mathcal{L}_{\text{kin}} = \frac{1}{2\bar{\Omega}^2} \left(1 + \frac{6\xi^2\bar{\phi}^2}{M_{\text{Pl}}^2\bar{\Omega}^2} \right) (\partial_\mu\hat{\phi})^2 + \frac{1}{2\bar{\Omega}^2} |\partial_\mu\pi|^2. \quad (4.5)$$

Thus, we further define the canonical fields $(\phi^{(E)}, \pi^{(E)})$ in Einstein frame via, $\hat{\phi} = \bar{\Omega}\bar{\zeta}\phi^{(E)}$ and $\pi = \bar{\Omega}\pi^{(E)}$, with the same $\bar{\zeta}$ in (4.2). Comparing the canonical fields in the two frames, we have, $\bar{\Omega} = \phi^{(J)}/\phi^{(E)} = \pi^{(J)}/\pi^{(E)}$, which amounts to a scale transformation for the fields.

4.2 Analysis of Scattering Amplitudes in Large Field Background

To study the amplitudes in large field background, we will generalize previous analysis to include all the relevant higher order ξ -dependent terms at $\mathcal{O}(E^2)$ under the $1/M_{\text{Pl}}$ expansion. We find that the calculations in Einstein frame are much simpler than that in Jordan frame. For the application to Higgs inflations in Sec. 4.3, we will focus on the analysis in Einstein frame. We will also comment on the case of Jordan frame in the end.

In Einstein frame, the analysis for large field background should include higher order terms of $\xi\bar{\phi}^2/M_{\text{Pl}}^2$ since they become $\mathcal{O}(1)$ at $\bar{\phi} \sim M_{\text{Pl}}/\sqrt{\xi}$. Thus, we generalize the formulation of Sec.2–3, and derive the scattering amplitudes in a generic background $\bar{\phi}$. By including the higher order contributions, the scalar interactions in (2.16) become,

$$\begin{aligned} \Delta\mathcal{L}_{\text{int}}^{ss} = & -\frac{q}{2v^2} \left(|\partial_\mu\pi|^2 + \zeta^2(\partial_\mu\phi)^2 \right) \left(|\pi|^2 + (1-4q)\zeta^2\phi^2 + 2v\zeta\phi \right) \\ & + \frac{1-\zeta^2}{8\zeta^2} \left(1 - \frac{2q}{v^2} (|\pi|^2 + \zeta^2\phi^2 + 2v\zeta\phi) + \frac{12q^2}{v^2}\zeta^2\phi^2 \right) \left[\partial_\mu \left(|\pi|^2 + \zeta^2\phi^2 + 2v\zeta\phi \right) \right]^2, \end{aligned} \quad (4.6)$$

where $q \equiv \xi v^2/M_{\text{Pl}}^2$, and we have rewritten the vertex coefficient $\xi^2 v^2/M_{\text{Pl}}^2$ in terms of ζ^2 . In Eq. (4.6), we only consider the operators involving cubic or quartic vertices. The Higgs-gauge interactions in (2.17) are replaced by

$$\Delta\mathcal{L}_{\text{int}}^{\phi q} = (2m_W^2 W_\mu^+ W^{\mu-} + m_Z^2 Z_\mu^2) \left[(1-q) \frac{\zeta}{v} \phi + (1-5q+4q^2) \frac{\zeta^2}{2v^2} \phi^2 \right]. \quad (4.7)$$

With these, we deduce general Feynman rules for the gauge and Goldstone boson scatterings. Derivation for pure Goldstone scattering amplitudes uses the same Feynman diagrams, while the Goldstone exchange should be further included for the processes with external Higgs bosons. As a generalization of Eq. (3.10), we rederive the full amplitudes at $\mathcal{O}(E^2)$ and for all electrically neutral channels,

$$\begin{aligned} \mathcal{T}(\pi^+\pi^- \rightarrow \pi^+\pi^-) &= [1 - (1-q)^2\zeta^2] (1 + \cos\theta) \frac{E^2}{2v^2}, \\ \mathcal{T}(\pi^+\pi^- \rightarrow \pi^0\pi^0) &= [1 - (1-q)^2\zeta^2] \frac{E^2}{v^2}, \\ \mathcal{T}(\pi^+\pi^- \rightarrow \phi\phi) &= (1-q) [3q + (1-\zeta^2)(1-2q) - q\zeta^2] \zeta^2 \frac{E^2}{v^2}, \\ \mathcal{T}(\pi^0\pi^0 \rightarrow \phi\phi) &= (1-q) [3q + (1-\zeta^2)(1-2q) - q\zeta^2] \zeta^2 \frac{E^2}{v^2}, \\ \mathcal{T}(\pi^0\phi \rightarrow \pi^0\phi) &= -(1-q) [3q + (1-\zeta^2)(1-2q) - q\zeta^2] (1 - \cos\theta) \zeta^2 \frac{E^2}{2v^2}. \end{aligned} \quad (4.8)$$

There are two elastic channels having no contributions at the $\mathcal{O}(E^2)$, i.e., $\mathcal{T}(\pi^0\pi^0 \rightarrow \pi^0\pi^0) \simeq \mathcal{T}(\phi\phi \rightarrow \phi\phi) = \mathcal{O}(E^0)$. Using the above generalized amplitudes, we have also verified the validity of equivalence theorem, which serves as nontrivial consistency checks of our calculation.

Next, we analyze the scattering amplitudes in a generic field background $\bar{\phi}$. Note that for Einstein frame v denotes VEV of $\phi^{(E)}$ in the electroweak vacuum. Considering the rescaling factor $\bar{\Omega}$ in (4.3), we can derive the new amplitudes from (4.8) via the replacements

$v \rightarrow \bar{\phi}/\bar{\Omega}$, $\zeta \rightarrow \bar{\zeta}$ and $q \rightarrow \bar{q}$ [cf. Eqs. (4.2)-(4.4)]. For the following sample processes, we have

$$\mathcal{T}(\pi^+\pi^-\rightarrow\pi^0\pi^0) = [1 - (1 - \bar{q})^2\bar{\zeta}^2] \bar{\Omega}^2 \frac{E^2}{\bar{\phi}^2}, \quad (4.9a)$$

$$\mathcal{T}(\pi^+\pi^-\rightarrow\phi\phi) = (1 - \bar{q}) [3\bar{q} + (1 - 2\bar{q})(1 - \bar{\zeta}^2) - \bar{q}\bar{\zeta}^2] \bar{\zeta}^2 \bar{\Omega}^2 \frac{E^2}{\bar{\phi}^2}. \quad (4.9b)$$

In the limit that $\bar{\phi} \ll M_{\text{Pl}}/\xi$, we have $(\bar{q}, \bar{\zeta}, \bar{\Omega})$ reduce to the quantities $(q, \zeta, 1)$ as defined in Sec. 2-3. But, the inflation epoch has $\bar{\phi} \gtrsim M_{\text{Pl}}/\sqrt{\xi}$, and thus corresponds to the different limits $\bar{q} \sim 1$ and $\bar{\zeta} \ll 1$ (for $\xi \gg 1$). This means that the previous expansion under $q \ll 1$ and $\zeta \sim 1$ no longer applies. In Einstein frame, for large $\bar{\phi}$ and $\xi \gg 1$, the exchange of graviton is always suppressed by $\bar{\zeta}^2$ as compared to the contributions of (4.9). For the sake of unitarity analysis in the background field $\bar{\phi} < M_{\text{Pl}}$, the graviton exchange is negligible.

Finally, we comment on the calculation in Jordan frame. For the scattering processes containing no Higgs boson in the in/out states, the calculation is straightforward. For instance, up to the constant rescaling for energy scale, the amplitude of $W_L^+ W_L^- \rightarrow Z_L^0 Z_L^0$ is the same as that in Einstein frame. At $\mathcal{O}(E^2)$, with negligible contribution from graviton exchange, the diagrams and Feynman vertices are the same. For the corresponding Goldstone scattering $\pi^+\pi^-\rightarrow\pi^0\pi^0$, we find that $\xi \neq 0$ contribution from graviton exchange equals that of contact interaction in Einstein frame. But there is a complication for scattering processes with external Higgs bosons. For both the cubic and quartic couplings of the Higgs and Goldstone bosons, the second order perturbative expansion of $\sqrt{-g}\mathcal{R}$ is needed to derive higher order terms in \bar{q} and $\bar{\zeta}^2$. This is more tedious than the first order expansion. In contrast, the Einstein frame has this complication transformed into higher dimensional operators of Higgs fields which are much easier to handle. Hence, we will perform the unitarity analysis for Higgs inflations in the Einstein frame.

4.3 Unitarity Constraints for Higgs Inflation

Now we use results of previous subsection to derive the perturbative unitarity bound for the Higgs inflation. In the conventional Higgs inflation model, the Higgs field couples to Ricci scalar through the nonminimal coupling (1.4) and plays the role of inflaton. During the inflation epoch, the background value of the unnormalized Higgs field $\hat{\phi}$ can be around $M_{\text{Pl}}/\sqrt{\xi}$, and the canonically normalized Higgs field ϕ will reach $\mathcal{O}(M_{\text{Pl}})$. In this case, the Higgs potential U in Einstein frame becomes exponentially flat when expressed in terms of canonically normalized background field χ ,

$$U \simeq \frac{\lambda M_{\text{Pl}}^4}{4\xi^2} \left(1 - e^{-\frac{2\chi}{\sqrt{6}M_{\text{Pl}}}}\right)^2. \quad (4.10)$$

At the classical level, the Planck normalization $(U/\epsilon)^{1/4} = 0.0276 M_{\text{Pl}}$ [35] requires $\xi \sim 10^4$ for $\lambda = \mathcal{O}(0.1)$, where ϵ is the first slow-roll parameter and is related to the tensor-to-scalar ratio $r = 16\epsilon$. The conventional Higgs inflation [7] has $\epsilon = r/16 \sim 1/N^2$ with N denoting the number of e -foldings. Thus, the typical choice of e -folding number $N = 50 - 60$ implies a fairly small ϵ and r , which agrees with the Planck data [35]. The inflation scale is defined as $\Lambda_{\text{INF}} = U^{1/4} \simeq \lambda^{1/4} M_{\text{Pl}}/\sqrt{\xi}$. Since the Higgs self-coupling $\lambda = \mathcal{O}(0.1)$, it is characterized by $\Lambda_{\text{INF}} \sim M_{\text{Pl}}/\sqrt{\xi}$.

On the other hand, the recent BICEP2 observation [24] on the large scale B-mode of CMB polarization suggests a rather large tensor-to-scalar ratio, $r = 0.20_{-0.05}^{+0.07}$. The BICEP2 results (if confirmed) will have important impact on Higgs inflation. While the typical parameter space of Higgs inflation predicts a quite small r as mentioned above, it is still possible to accommodate a sizable r , as discussed in [21–23], through the tuning of top quark mass or proper extensions of the model. Due to the renormalization group running, the Higgs self-coupling λ becomes extremely small at the inflation scale, at which a not-so-flat region of the Higgs potential is realized. Then, only a mildly large $\xi \sim 10$ is needed to further flatten the potential. Since the shape of the potential is no longer exponential, the tensor-to-scalar ratio r can be sizable. This scenario uses the Einstein-frame Higgs field to set the renormalization scale. Alternatively, one may use the Jordan-frame Higgs field, and this approach can result in a quadratic chaotic inflation in Einstein frame [21]. In this case, the nonminimal coupling is required to be $\xi \sim 100$. We note that for either case, the inflation scale is generally fixed by inputting the BICEP2 data on r via $\epsilon = r/16$. Thus, we have, $\Lambda_{\text{INF}} = U^{1/4} \simeq 2.3 \times 10^{16}$ GeV, which coincides with the conventional grand unification (GUT) scale. Hence, Λ_{INF} is much lower than $M_{\text{Pl}}/\sqrt{\xi}$ for $\xi = \mathcal{O}(10 - 100)$.

In all cases above, we see that the nonminimal coupling in Higgs inflations is significantly larger than one, $\xi > 1$. Thus, a typical inflation scale such as $M_{\text{Pl}}/\sqrt{\xi}$ will be apparently higher than our unitarity bound of $\mathcal{O}(M_{\text{Pl}}/\xi)$ as given in Eq. (3.20) [Sec. 3.3], and we may worry about the unitarity issue of perturbative analysis of Higgs inflation. But, as discussed above, the background value of Higgs field during inflation is very large. This means that we should rederive the unitarity bound for scattering amplitudes with large background, rather than using the result of Sec. 3.3. Since we have systematically derived the scattering amplitudes with large background in the previous subsection, we are now ready to analyze the background-dependent unitarity constraints on the Higgs inflation models. The use of flat-spacetime amplitudes in nearly de Sitter background during inflation is justified, because the scale of spacetime curvature (as characterized by the Hubble parameter $H \sim 10^{14}$ GeV) is smaller than the inflation scale 10^{16} GeV (as inferred from the energy density) by two orders of magnitude, according to the Friedmann equation.

Let us first study the unitarity bounds for the representative scattering channels. We impose $|\Re a_0| < 1/2$ for the amplitudes in (4.9) after proper normalization of their initial/final states. Thus, we compute the unitarity limits $\Lambda_{\pi\pi}^{(E)}$ and $\Lambda_{\phi\phi}^{(E)}$ for $\pi^+\pi^- \rightarrow \pi^0\pi^0$ and $\pi^+\pi^- \rightarrow \phi\phi$, respectively,

$$\Lambda_{\pi\pi}^{(E)} = \left(\frac{8\sqrt{2}\pi}{1 - (1 - \bar{q})^2 \bar{\zeta}^2} \right)^{\frac{1}{2}} \frac{\bar{\phi}}{\bar{\Omega}}, \quad (4.11a)$$

$$\Lambda_{\phi\phi}^{(E)} = \left(\frac{8\sqrt{2}\pi}{(1 - \bar{q}) [3\bar{q} + (1 - 2\bar{q})(1 - \bar{\zeta}^2) - \bar{q}\bar{\zeta}^2]} \right)^{\frac{1}{2}} \frac{\bar{\phi}}{\bar{\zeta}\bar{\Omega}}. \quad (4.11b)$$

Considering the LHC constraint $|\xi| < (2.7 - 5.2) \times 10^{15}$ from Fig. 4, we have $\xi v^2 \ll M_{\text{Pl}}^2$, and thus $M^2 \simeq M_{\text{Pl}}^2$. This gives, $\bar{M}_{\text{Pl}}^2 \simeq M_{\text{Pl}}^2 + \xi \bar{\phi}^2$. Hence, for $\xi \gg 1$, we can derive the following asymptotic behaviors,

$$\Lambda_{\pi\pi}^{(E)} \sim \begin{cases} \frac{M_{\text{Pl}}}{\xi}, & \bar{\phi} \ll \frac{M_{\text{Pl}}}{\xi}, \\ \bar{\phi}, & \frac{M_{\text{Pl}}}{\xi} \ll \bar{\phi} \ll \frac{M_{\text{Pl}}}{\sqrt{\xi}}, \\ \frac{M_{\text{Pl}}}{\sqrt{\xi}}, & \bar{\phi} \gg \frac{M_{\text{Pl}}}{\sqrt{\xi}}, \end{cases} \quad \Lambda_{\phi\phi}^{(E)} \sim \begin{cases} \frac{M_{\text{Pl}}}{\xi}, & \bar{\phi} \ll \frac{M_{\text{Pl}}}{\xi}, \\ \frac{\xi \bar{\phi}^2}{M_{\text{Pl}}}, & \frac{M_{\text{Pl}}}{\xi} \ll \bar{\phi} \ll \frac{M_{\text{Pl}}}{\sqrt{\xi}}, \\ \sqrt{\xi} \bar{\phi}, & \bar{\phi} \gg \frac{M_{\text{Pl}}}{\sqrt{\xi}}. \end{cases} \quad (4.12)$$

For completeness, we also remark that in the case of⁵ $M^2 \ll M_{\text{Pl}}^2$, we would have $\Lambda_{\pi\pi}^{(E)} \sim M_{\text{Pl}}/\sqrt{\xi}$ and $\Lambda_{\phi\phi}^{(E)} \sim (M_{\text{Pl}}/M)\sqrt{\xi}\bar{\phi} \gg \sqrt{\xi}\bar{\phi}$.

To study the the unitarity constraints on Higgs inflation, we present in Fig. 7 the unitarity bound $\Lambda^{(E)}$ as a function of $\bar{\phi}$, with sample inputs $\xi = 10^4$ [plot-(a)], $\xi = 10^2$ [plot-(b)], and $\xi = 10$ [plot-(c)]. For clarity, we normalize both axes by Λ_{INF} in each plot. The red and blue curves denote the unitarity bounds $\Lambda_{\pi\pi}^{(E)}$ and $\Lambda_{\phi\phi}^{(E)}$, respectively. The light pink and blue areas above each curve violate perturbative unitarity. Plot-(a) demonstrates the conventional Higgs inflation [7] with a large $\xi = 10^4$. The inflation scale $\Lambda_{\text{INF}} \simeq M_{\text{Pl}}/\sqrt{\xi}$ is depicted as the horizontal dashed line. It shows that the strongest unitarity bound is higher than the effective inflation scale $M_{\text{Pl}}/\sqrt{\xi}$ for $\bar{\phi} \gtrsim 0.2\Lambda_{\text{INF}}$. This agrees well with the schematic picture from recent qualitative estimates [13]. Plots (b) and (c) represent the improved models [21–23] compatible with a large r as indicated by the BICEP2 observation [24]. For illustration, we set $\xi = 10^2$ and $\xi = 10$ for the two sample scenarios discussed above. Here, the inflation scale $\Lambda_{\text{INF}} \simeq 2.3 \times 10^{16}$ GeV is denoted by the horizontal dashed line at the ratio $\Lambda^{(E)}/\Lambda_{\text{INF}} = 1$. It is lower than the unitarity bound even for the small background field regions. This shows that the unitarity constraints are largely relieved for moderate values of the nonminimal coupling, $\xi = \mathcal{O}(10 - 100)$.

⁵The limit $M^2 \rightarrow 0$ leads to $M_{\text{Pl}}^2 = \xi v^2$. This corresponds to the early scenarios of induced gravity inflation [36].

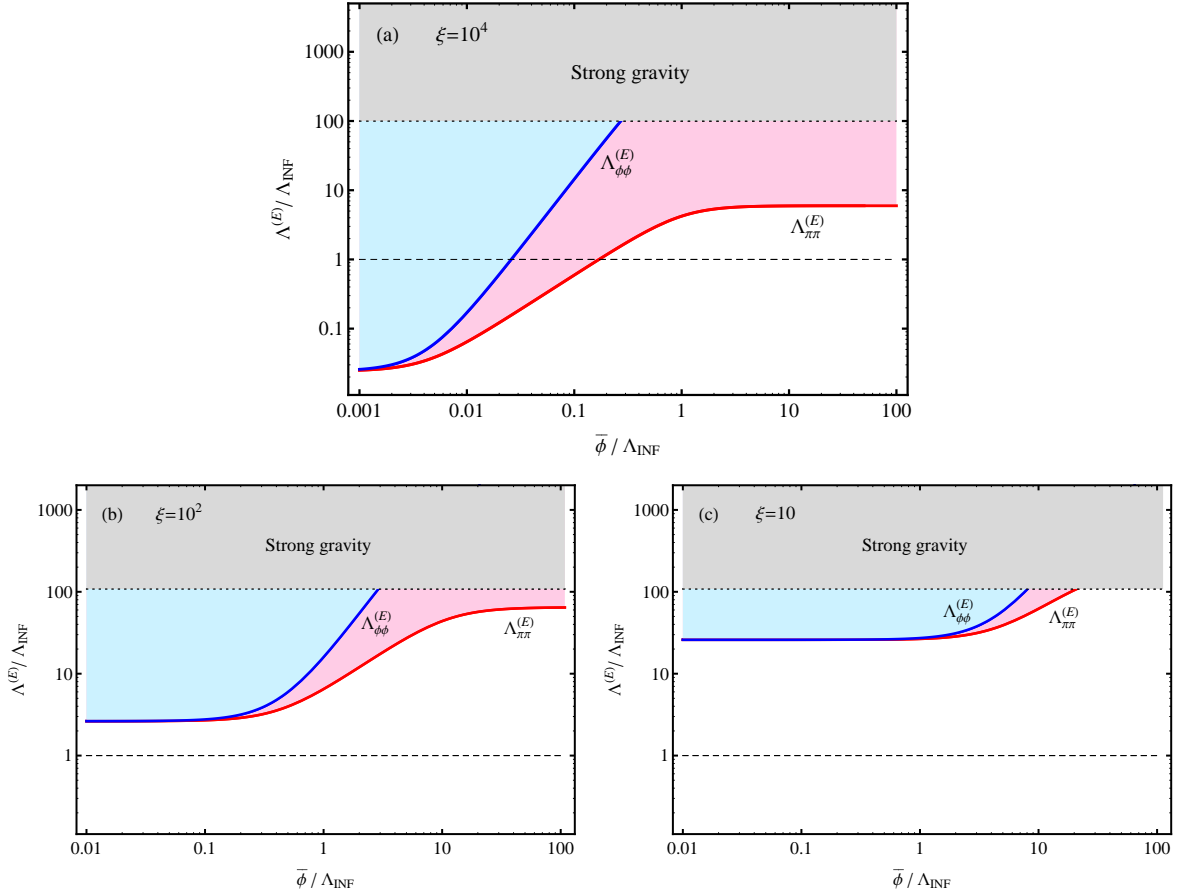


Figure 7. Perturbative unitarity bounds $\Lambda^{(E)}$ as functions of $\bar{\phi}$, with $\xi = 10^4$ [plot-(a)], $\xi = 10^2$ [plot-(b)] and $\xi = 10$ [plot-(c)]. Here, both axes are normalized by Λ_{INF} . In all plots, the blue and red curves denote $\Lambda_{\phi\phi}^{(E)}$ and $\Lambda_{\pi\pi}^{(E)}$, respectively, where the region above each curve violates perturbative unitarity. The grey area with dotted boundary denotes the strong gravity region, which is above the reduced Planck mass M_{Pl} . The horizontal dashed line denotes the inflation scale $\Lambda_{\text{INF}} \simeq M_{\text{Pl}}/\sqrt{\xi}$ in plot-(a), and $\Lambda_{\text{INF}} \simeq 2.3 \times 10^{16}$ GeV in plot-(b,c) as indicated by the BICEP2 data.

In parallel with the perturbative unitarity bound (3.20) derived in the electroweak vacuum in Sec. 3.3, we perform a coupled channel analysis for the large field background $\bar{\phi} \gtrsim M_{\text{Pl}}/\sqrt{\xi}$. For the four neutral channels, $|\pi^+\pi^- \rangle$, $\frac{1}{\sqrt{2}}|\pi^0\pi^0 \rangle$, $\frac{1}{\sqrt{2}}|\phi\phi \rangle$, and $|\pi^0\phi \rangle$, we deduce the s -wave amplitudes,

$$a_0(E) = \frac{[1 - (1 - \bar{q})^2 \bar{\zeta}^2] \bar{\Omega}^2 E^2}{32\pi \bar{\phi}^2} \begin{pmatrix} 1 & \sqrt{2} & \sqrt{2}A & 0 \\ \sqrt{2} & 0 & A & 0 \\ \sqrt{2}A & A & 0 & 0 \\ 0 & 0 & 0 & -A \end{pmatrix}$$

$$\simeq \frac{\bar{\Omega}^2 E^2}{32\pi\bar{\phi}^2} \begin{pmatrix} 1 & \sqrt{2} & 0 & 0 \\ \sqrt{2} & 0 & 0 & 0 \\ 0 & 0 & 0 & 0 \\ 0 & 0 & 0 & 0 \end{pmatrix}. \quad (4.13)$$

In the above, we have denoted,

$$A = \frac{1 + \bar{q} - (1 - \bar{q})\bar{\zeta}^2}{1 - (1 - \bar{q})^2\bar{\zeta}^2} \frac{\bar{\zeta}^2}{\bar{\Omega}^2}. \quad (4.14)$$

For the large background field $\bar{\phi} \sim M_{\text{Pl}}/\sqrt{\xi}$ and large $\xi \gg 1$, we have the asymptotic behavior $A \sim \xi^{-1} \ll 1$, and thus the A term is negligible for the current analysis. This means that the processes with Higgs bosons in the external states have negligible contribution. Imposing the unitarity condition on the largest eigenvalue of a_0 via the above coupled channel analysis, we infer the unitarity bound for large background field $\bar{\phi}$,

$$E < 2^{-\frac{1}{4}} \Lambda_{\pi\pi}^{(E)}, \quad (4.15)$$

where $\Lambda_{\pi\pi}^{(E)}$ is given by (4.11a). For comparison, we present this bound in the $(E, |\xi|)$ plane at $\bar{\phi} = M_{\text{Pl}}/\sqrt{\xi}$ in Fig. 4(b) by the red curve, where the yellow region violates perturbative unitarity. It shows that the unitarity bound is significantly relieved when derived in the large field background, which applies to the case of Higgs inflation. In the same plot-(b) of Fig. 4, we draw a vertical dashed line to depict the inflation scale, $\Lambda_{\text{INF}} \simeq 2.3 \times 10^{16}$ GeV, as indicated by the BICEP2 data [24]. For the scattering energy around the inflation scale, $E \sim \Lambda_{\text{INF}}$, we see that the red curve imposes a unitarity bound, $\xi < \mathcal{O}(10^{5-6})$.

Finally, for comparison with the literature, we note that the interesting papers [13] discussed two types of unitarity bounds for both frames by simple power counting analysis. It estimated the unitarity bound $\Lambda_{\text{g-s}}$ for scalar-gravity coupling of $\phi - \phi - h_{\mu\nu}$ in the Jordan frame, which contributes to the process $\phi\phi \rightarrow \phi\phi$. As we showed earlier, this specific scattering amplitude has vanishing E^2 term due to the crossing symmetry of (s, t, u) channels. It also estimated the unitarity bound Λ_{gauge} from the gauge boson scattering. These estimates [13] agree with the main feature of our quantitative unitarity bounds $\Lambda_{\pi\pi}$ in (4.11) and Fig. 7. As shown above, the $\Lambda_{\pi\pi}^{(E)}$ places the best unitarity constraint over the large background field region of the Higgs inflation. Recently, Ref. [37] studied the impact of UV physics on the prediction of Higgs inflation. They utilized the non-linear realization to discuss the unitarity of Higgs inflation, and derived the leading order Goldstone amplitudes, which are in qualitative agreement with our results. We have also derived the scattering amplitude with Higgs bosons as external states. Furthermore, we presented the quantitative unitarity bounds on the Higgs inflation models in Fig. 7(a)-(c).

5 Conclusions

It is striking that the gravitational force not only shapes the world at its macroscopic and cosmological scales, but will also play key role at the fundamental Planck scale. We would then ask: *what happens in between?* Given the LHC discovery of a 125 GeV Higgs boson [1, 2], it is strongly motivated for us to explore the Higgs gravitational interactions in connection with the electroweak symmetry breaking mechanism and the origin of inertial mass generation for all elementary particles, as well as the Higgs inflation.

Combining the SM with general relativity (GR) as a joint effective theory, we note that there is a unique dimension-4 operator (1.4) for the Higgs-gravity interactions with nonminimal coupling ξ . This provides a generic Higgs portal to the new physics beyond SM. In this work, we systematically studied the contributions of this Higgs-gravity interaction (1.4) to weak boson scattering processes in both Jordan and Einstein frames, over the energy regions accessible by the LHC (14 TeV) and the future circular pp colliders (50–100 TeV). We explicitly demonstrated the equivalence theorem in the presence of Higgs-gravity coupling ξ in both Jordan and Einstein frames. For the ξ -induced leading amplitudes, we derived the full results at $\mathcal{O}(E^2)$, which are needed for studying the case of large background field in Higgs inflations. Then, we analyzed the perturbative unitarity bound on ξ via coupled channel analysis in the background of the electroweak vacuum. We also verified the equivalence between the two frames for computing the scattering amplitudes and cross sections. This systematically extends our previous short study [15] with analysis in the Einstein frame alone and only to the first order of $1/M_{\text{Pl}}^2$. For applications to Higgs inflation, we further studied the weak boson scatterings and unitarity constraints for the large background field case. We quantitatively established the viable perturbative parameter space of the conventional Higgs inflation [7] and the improved models [21, 22] in light of the recent BICEP2 data [24].

To be concrete, in Sec. 2 we presented the formulation in Jordan and Einstein frames. We derived the ξ -induced Higgs-gravity interactions for both frames, and summarized all the relevant Feynman rules in Appendix A. Then, in Sec. 3 we systematically analyzed longitudinal weak boson scattering and the corresponding Goldstone boson scattering in both frames. In each frame, we explicitly demonstrated the longitudinal-Goldstone boson equivalence theorem with nonzero Higgs-gravity coupling ξ . We further verified the equivalence between the two frames for all scattering processes. In Sec. 3.3, we performed a coupled channel analysis of weak boson scattering in the electroweak vacuum, and derived unitarity bound on ξ in Fig. 4. We further studied two intriguing scenarios, in which the UV cutoff for the SM + GR effective theory is around $\Lambda_{\text{UV}} = \mathcal{O}(10 \text{ TeV})$ and $\Lambda_{\text{UV}} = \mathcal{O}(50 \text{ TeV})$, respectively. Thus, the ξ coupling can reach up to $\xi = \mathcal{O}(10^{15})$ for $\Lambda_{\text{UV}} = \mathcal{O}(10 \text{ TeV})$, or, reach up

to $\xi = \mathcal{O}(10^{14})$ for $\Lambda_{\text{UV}} = \mathcal{O}(50 \text{ TeV})$, as shown in Fig. 4(a). In Fig. 5, we presented our predictions of the WW scattering cross sections with coupling $\xi = \mathcal{O}(10^{15})$, over the energy scale $E(WW) = 0.2 - 4 \text{ TeV}$, which is accessible at the LHC (14 TeV). These exhibit *different behaviors* from the naive SM result ($\xi = 0$), and thus will be discriminated by the upcoming runs at the LHC (14 TeV) with higher integrated luminosity. We further analyzed the WW scattering cross sections in the energy range of $E(WW) = 1 - 30 \text{ TeV}$. These will be realized at the future circular pp colliders (50 – 100 TeV) [25], which may have sensitivity to probe the Higgs-gravity coupling at the level of $\xi = \mathcal{O}(10^{14})$, as shown in Fig. 6. We suggest that the ξ coupling can be further probed by invoking the cubic Higgs self-interactions [Eq. (2.16)] at the future high energy pp colliders.

In Sec. 4, we studied the Higgs-field-background dependent weak boson scattering amplitudes, and quantitatively performed the unitarity analysis for the Higgs inflation models. We generalized the formulation of Sec. 2 to a generic Higgs-field background in both Jordan and Einstein frames. We derived the new Feynman rules and the scattering amplitudes accordingly. For the case of large field background, we have taken account of the full contributions at $\mathcal{O}(E^2)$ for the scattering amplitudes. With these, we demonstrated that the unitarity bound on the ξ coupling is substantially relieved, as shown in Fig. 4(b). Finally, we applied this analysis to the conventional Higgs inflation [7] and the improved models [21, 22] in light of the recent BICEP2 observation [24]. We quantitatively analyzed the viable perturbative parameter space for the Higgs inflation models, as shown in Fig. 7(a)-(c) for three sample inputs of the ξ coupling.

Acknowledgements

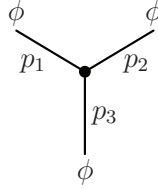
We thank John R. Ellis for valuable discussions during his recent visit at Tsinghua HEP Center. We thank Michael Trott and Xavier Calmet for valuable discussions on this subject. This work was supported by National NSF of China (under grants 11275101, 11135003) and National Basic Research Program (under grant 2010CB833000).

Appendix

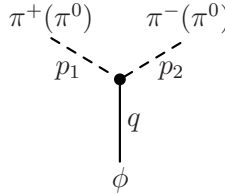
A Feynman Rules in Jordan and Einstein Frames

In this appendix, we present all the relevant Feynman rules at $\mathcal{O}(M_{\text{Pl}}^{-2})$ in the electroweak vacuum for evaluating longitudinal and Goldstone boson scattering in both Jordan and Einstein frames. We have retained the rescaling factor ζ for the Higgs field ϕ without expansion. This will also allow us to extract the leading terms of $(\xi v/M_{\text{Pl}})^{2n}$ for the scattering amplitudes at $\mathcal{O}(E^2)$. In our notation, all momenta will flow inward.

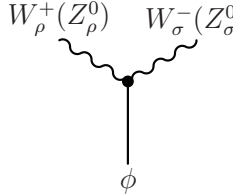
A.1 Feynman Rules in Jordan Frame



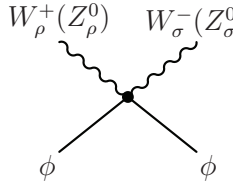
$$= -i6\zeta^3\lambda v + \zeta^3\left(-\frac{i\xi v}{M_{\text{Pl}}^2} + \frac{i6\xi^2 v}{M_{\text{Pl}}^2}\right)(p_1^2 + p_2^2 + p_3^2). \quad (\text{A.1})$$



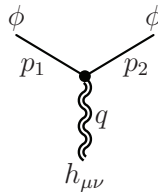
$$= -i2\lambda\zeta v + \frac{i2\xi\zeta v}{M_{\text{Pl}}^2}(p_1 \cdot p_2) + \frac{i6\xi^2\zeta v}{M_{\text{Pl}}^2}q^2, \quad (\text{A.2})$$



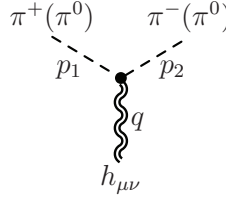
$$= \frac{i2m_{W(Z)}^2}{v}\left(1 - \frac{\xi v^2}{M_{\text{Pl}}^2}\right)\zeta\eta^{\rho\sigma}, \quad (\text{A.3})$$



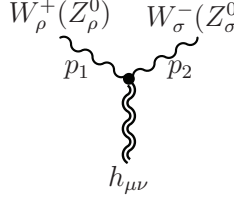
$$= \frac{i2m_{W(Z)}^2}{v^2}\left(1 - \frac{4\xi v^2}{M_{\text{Pl}}^2}\right)\zeta^2\eta^{\rho\sigma}, \quad (\text{A.4})$$



$$= \frac{i\sqrt{2}}{M_{\text{Pl}}}\zeta^2\left[\xi(q^\mu q^\nu - q^2\eta^{\mu\nu}) + (p_1^{(\mu} p_2^{\nu)} - \frac{1}{2}p_1 \cdot p_2\eta^{\mu\nu})\right], \quad (\text{A.5})$$

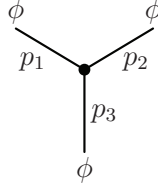


$$= \frac{i\sqrt{2}}{M_{\text{Pl}}} \left[\xi(q^\mu q^\nu - q^2 \eta^{\mu\nu}) + (p_1^{(\mu} p_2^{\nu)} - \frac{1}{2} p_1 \cdot p_2 \eta^{\mu\nu}) \right], \quad (\text{A.6})$$

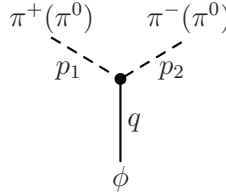


$$= -\frac{i\sqrt{2}}{M_{\text{Pl}}} \left[p_1^{(\mu} p_2^{\nu)} \eta^{\rho\sigma} + \frac{1}{2} p_1^\sigma p_2^\rho \eta^{\mu\nu} - p_1^\sigma p_2^{(\nu} \eta^{\mu)\rho} - p_2^\rho p_1^{(\mu} \eta^{\nu)\sigma} \right. \\ \left. + (p_1 \cdot p_2 + m_{W,Z}^2) (\eta^{\rho(\mu} \eta^{\nu)\sigma} - \frac{1}{2} \eta^{\mu\nu} \eta^{\rho\sigma}) \right]. \quad (\text{A.7})$$

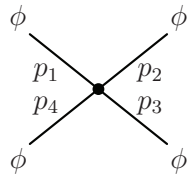
A.2 Feynman Rules in Einstein Frame



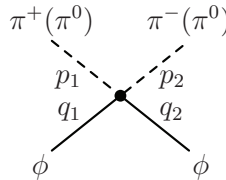
$$= -i6\zeta^3 \lambda v + \zeta^3 \left(-\frac{i\xi v}{M_{\text{Pl}}^2} + \frac{i6\xi^2 v}{M_{\text{Pl}}^2} \right) (p_1^2 + p_2^2 + p_3^2), \quad (\text{A.8})$$



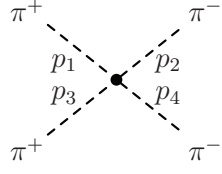
$$= -i2\lambda\zeta v + \frac{i2\xi\zeta v}{M_{\text{Pl}}^2} (p_1 \cdot p_2) + \frac{i6\xi^2\zeta v}{M_{\text{Pl}}^2} q^2, \quad (\text{A.9})$$



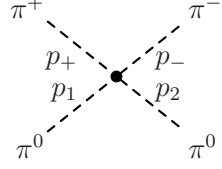
$$= -i6\lambda\zeta^4 + \frac{i2\xi\zeta^4}{M_{\text{Pl}}^2} (p_1 \cdot p_2 + 5 \text{ permutations}) \\ + \frac{i3\xi^2\zeta^4}{M_{\text{Pl}}^2} [(p_1 + p_2)^2 + 5 \text{ permutations}], \quad (\text{A.10})$$



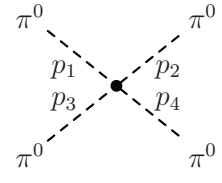
$$= -i\lambda\zeta^2 + \frac{i2\xi\zeta^2}{M_{\text{Pl}}^2} (p_1 \cdot p_2 + q_1 \cdot q_2) + \frac{i6\xi^2\zeta^2}{M_{\text{Pl}}^2} (p_1 + p_2)^2, \quad (\text{A.11})$$



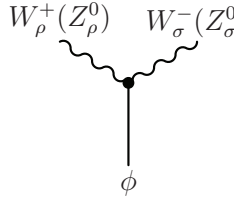
$$= -i2\lambda - \frac{i2\xi}{M_{\text{Pl}}^2}(p_1 + p_3)^2 + \frac{i6\xi^2}{M_{\text{Pl}}^2} [(p_1 + p_2)^2 + (p_1 + p_4)^2], \quad (\text{A.12})$$



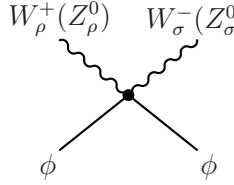
$$= -i2\lambda + \frac{2i\xi}{M_{\text{Pl}}^2}(p_+ \cdot p_- + p_1 \cdot p_2) + \frac{i6\xi^2}{M_{\text{Pl}}^2}(p_+ + p_-)^2, \quad (\text{A.13})$$



$$= -i6\lambda + \frac{i2\xi}{M_{\text{Pl}}^2}(p_1 \cdot p_2 + 5 \text{ permutations}) + \frac{i3\xi^2}{M_{\text{Pl}}^2} [(p_1 + p_2)^2 + 5 \text{ permutations}], \quad (\text{A.14})$$



$$= \frac{i2m_{W(Z)}^2}{v} \left(1 - \frac{\xi v^2}{M_{\text{Pl}}^2}\right) \zeta \eta^{\rho\sigma}, \quad (\text{A.15})$$



$$= \frac{i2m_{W(Z)}^2}{v^2} \left(1 - \frac{5\xi v^2}{M_{\text{Pl}}^2}\right) \zeta^2 \eta^{\rho\sigma}. \quad (\text{A.16})$$

References

- [1] G. Aad *et al.* (ATLAS Collaboration), *Observation of a new particle in the search for the Standard Model Higgs boson with the ATLAS detector at the LHC*, Phys. Lett. B **716** (2012) 1 [arXiv:1207.7214 [hep-ex]]; S. Chatrchyan *et al.* (CMS Collaboration), *Observation of a new boson at a mass of 125 GeV with the CMS experiment at the LHC*, Phys. Lett. B **716** (2012) 30 [arXiv:1207.7235 [hep-ex]].
- [2] ATLAS and CMS Collaborations, B. Di Micco, *Combinations of Results of Higgs Production in all Decay Channels at LHC*, at *XLIX Rencontres de Moriond 2014: QCD and High Energy Interactions*, March 22-29, 2014, Moriond, La Thuile, Italy.
- [3] E.g., M. E. Peskin, *Estimation of LHC and ILC Capabilities for Precision Higgs Boson Coupling Measurements*, arXiv:1312.4974; and W. Yao, *Studies of Measuring Higgs Self-coupling with $HH \rightarrow b\bar{b}\gamma\gamma$ at the Future Hadron Colliders*, arXiv:1308.6302, in the proceedings of the Snowmass Community Summer Study, July 29–Aug. 26, 2013, Minneapolis, MN, USA; M. Bicer *et al.*, *First Look at the Physics Case of TLEP*, JHEP **1401** (2014) 164 [arXiv:1308.6176 [hep-ex]]; and references therein.
- [4] G. 't Hooft and M. J. G. Veltman, *One Loop Divergencies in the Theory of Gravitation*, Ann. Poincaré Phys. Theor. A **20** (1974) 69; S. Deser and P. van Nieuwenhuizen, *One Loop Divergences of Quantized Einstein-Maxwell Fields*, Phys. Rev. D **10** (1974) 401; S. Deser, H. S. Tsao, P. van Nieuwenhuizen, *One Loop Divergences of the Einstein Yang-Mills System*, Phys. Rev. D **10** (1974) 3337.
- [5] For a recent review of effective field theory, S. Weinberg, *Effective Field Theory, Past and Future*, PoS CD 09 (2009) 001 [arXiv:0908.1964 [hep-th]]; and references therein.
- [6] For reviews, S. D. Odintsov, *Renormalization Group, Effective Action and Grand Unification Theories in Curved Space-time*, Fortsch. Phys. **39** (1991) 621; I. L. Buchbinder, S. D. Odintsov, and I. L. Shapiro, *Effective Action in Quantum Gravity*, published in Bristol, UK, IOP (1992); and references therein.
- [7] F. L. Bezrukov and M. Shaposhnikov, *The Standard Model Higgs Boson as the Inflaton*, Phys. Lett. B **659** (2008) 703 [arXiv:0710.3755].
- [8] A. O. Barvinsky, A. Y. Kamenshchik, and A. A. Starobinsky, *Inflation Scenario via the Standard Model Higgs Boson and LHC*, JCAP **0811** (2008) 021 [arXiv:0809.2104].
- [9] A. De Simone, M. P. Hertzberg, and F. Wilczek, *Running Inflation in the Standard Model*, Phys. Lett. B **678** (2009) 1 [arXiv:0812.4946].
- [10] A. O. Barvinsky, A. Y. Kamenshchik, C. Kiefer, A. A. Starobinsky, and C. Steinwachs, *Asymptotic Freedom in Inflationary Cosmology with a Non-minimally Coupled Higgs Field*, JCAP **0912** (2009) 003 [arXiv:0904.1698 [hep-ph]].
- [11] A. O. Barvinsky, A. Y. Kamenshchik, C. Kiefer, A. A. Starobinsky, and C. F. Steinwachs, *Higgs Boson, Renormalization Group, and Naturalness in Cosmology*, Eur. Phys. J. C **72** (2012) 2219 [arXiv:0910.1041 [hep-ph]].
- [12] F. Bezrukov, A. Magnin, M. Shaposhnikov, and S. Sibiryakov, *Higgs Inflation: Consistency and Generalisations*, JHEP **1101** (2011) 016 [arXiv:1008.5157].
- [13] F. Bezrukov, *The Higgs Field as an Inflaton*, Class. Quant. Grav. **30** (2013) 214001 [arXiv:1307.0708]; and references therein.
- [14] M. Atkins and X. Calmet, *Bounds on the Nonminimal Coupling of the Higgs Boson to Gravity*, Phys. Rev. Lett. **110** (2013) 051301 [arXiv:1211.0281].
- [15] Z. Z. Xianyu, J. Ren, and H. J. He, *Gravitational Interaction of Higgs Boson and Weak Boson Scattering*, Phys. Rev. D **88** (2013) 096013 [arXiv:1305.0251].

- [16] For a comprehensive review of the longitudinal-Goldstone equivalence theorem, H. J. He, Y. P. Kuang, C. P. Yuan, *Global Analysis for Probing Electroweak Symmetry Breaking Mechanism at High Energy Colliders*, DESY-97-056 [arXiv:hep-ph/9704276], and references therein.
- [17] For a review of this subject, V. Faraoni, E. Gunzig, and P. Nardone, *Conformal Transformations in Classical Gravitational Theories and in Cosmology*, *Fund. Cosmic Phys.* **20** (1999) 121 [arXiv:gr-qc/9811047]; and references therein.
- [18] F. Bezrukov and M. Shaposhnikov, *Standard Model Higgs Boson Mass from Inflation: Two Loop Analysis*, *JHEP* **0907** (2009) 089 [arXiv:0904.1537 [hep-ph]].
- [19] D. P. George, S. Mooij, and M. Postma, *Quantum Corrections in Higgs Inflation: the Real Scalar Case*, *JCAP* **1402** (2014) 024 [arXiv:1310.2157]; and references therein.
- [20] For a partial list, e.g., C. P. Burgess, H. M. Lee, and M. Trott, *Power-counting and the Validity of the Classical Approximation During Inflation* *JHEP* **0909** (2009) 103 [arXiv:0902.4465]; J. L. F. Barbon and J. R. Espinosa, *On the Naturalness of Higgs Inflation*, *Phys. Rev. D* **79** (2009) 081302 [arXiv:0903.0355]; C. P. Burgess, H. M. Lee, and M. Trott, *Comment on Higgs Inflation and Naturalness*, *JHEP* **1007** (2010) 007 [arXiv:1002.2730]; R. N. Lerner and J. McDonald, *Higgs Inflation and Naturalness*, *JCAP* **1004** (2010) 015 [arXiv:0912.5463]; *Unitarity violation in Generalized Higgs Inflation Models*, *JCAP* **1211** (2012) 019 [arXiv:1112.0954]; M. P. Hertzberg, *On Inflation with Non-minimal Coupling*, *JHEP* **1011** (2010) 023 [arXiv:1002.2995]; G. F. Giudice and H. M. Lee, *Unitarizing Higgs Inflation*, *Phys. Lett. B* **694** (2011) 294 [arXiv:1010.1417]; M. Atkins and X. Calmet, *Remarks on Higgs Inflation*, *Phys. Lett. B* **697** (2011) 37 [arXiv:1011.4179]; O. Lebedev and H. M. Lee, *Higgs Portal Inflation*, *Eur. Phys. J. C* **71** (2011) 1821 [arXiv:1105.2284]; M. Rinaldi, *The dark aftermath of Higgs inflation*, *Eur. Phys. J. Plus* **129** (2014) 56 [arXiv:1309.7332]; C. P. Burgess, S. P. Patil, and M. Trott, *On the Predictiveness of Single-Field Inflationary Models*, arXiv:1402.1476 [hep-ph]; and references therein.
- [21] Y. Hamada, H. Kawai, K. Y. Oda, and S. C. Park, *Higgs Inflation Still Alive*, *Phys. Rev. Lett.* (2014), arXiv:1403.5043 [hep-ph]; K. Allison, *Higgs ξ -Inflation for the 125 – 126 GeV Higgs: a Two-loop Analysis*, *JHEP* **1402** (2014) 040 [arXiv:1306.6931 [hep-ph]].
- [22] F. Bezrukov and M. Shaposhnikov, *Higgs inflation at the critical point*, arXiv:1403.6078 [hep-ph].
- [23] N. Haba and R. Takahashi, *Higgs Inflation with Singlet Scalar Dark Matter and Right-handed Neutrino in the Light of BICEP2*, arXiv:1404.4737 [hep-ph].
- [24] P. A. R. Ade *et al.*, [BICEP2 Collaboration], *BICEP2 I: Detection of B-mode Polarization at Degree Angular Scales*, [arXiv:1403.3985 [astro-ph.CO]].
- [25] E.g., see presentations at the Kickoff Meeting of Future Circular Collider Study, Feb. 12-15, 2014, Geneva, Switzerland; and the International Workshop on Future High Energy Circular Colliders December 16-17, 2013, IHEP, Beijing, China; M. Bicer *et al.*, [TLEP Working Group], *First Look at the Physics Case of TLEP*, *JHEP* **1401** (2014) 164 [arXiv:1308.6176 [hep-ex]], and references therein.
- [26] M. Atkins and X. Calmet, *Unitarity bounds on low scale quantum gravity*, *Eur. Phys. J. C* **70** (2010) 381 [arXiv:1005.1075]; *On the unitarity of linearized General Relativity coupled to matter*, *Phys. Lett. B* **695** (2011) 298 [arXiv:1002.0003]; T. Han and S. Willenbrock, *Scale of quantum gravity*, *Phys. Lett. B* **616** (2005) 215 [hep-ph/0404182]; and references therein.
- [27] S. Coleman, J. Wess, and B. Zumino, *Structure of Phenomenological Lagrangians 1*, *Phys. Rev.* **177** (1969) 2239; C. G. Callan, S. Coleman, J. Wess, and B. Zumino, *Structure of Phenomenological Lagrangians 2*, *Phys. Rev.* **177** (1969) 2247; and references therein.
- [28] J. M. Cornwall, D. N. Levin, and G. Tiktopoulos, *Uniqueness of Spontaneously Broken Gauge*

- Theories*, Phys. Rev. Lett. **30** (1973) 1268; *Derivation of Gauge Invariance from High-Energy Unitarity Bounds on the S Matrix*, Phys. Rev. D **10** (1974) 1145 [Erratum, D **11** (1975) 972].
- [29] D. A. Dicus and V. S. Mathur, *Upper Bounds on the Values of Masses in Unified Gauge Theories*, Phys. Rev. D **7** (1973) 3111; C. H. Llewellyn Smith, *High-Energy Behavior and Gauge Symmetry*, Phys. Lett. **46B** (1973) 233.
- [30] B. W. Lee, C. Quigg and H. B. Thacker, *Weak Interactions at Very High Energies: The Role of the Higgs Boson Mass*, Phys. Rev. D **16** (1977) 1519; *The Strength of Weak Interactions at Very High Energies and the Higgs Boson Mass*, Phys. Rev. Lett. **38** (1977) 883.
- [31] M. S. Chanowitz and M. K. Gaillard, *The TeV Physics of Strongly Interacting W's and Z's*, Nucl. Phys. B **261** (1985) 379. For a review, M. S. Chanowitz, *The No-Higgs Signal: Strong WW Scattering at the LHC*, Czech. J. Phys. **55** (2005) B45 [arXiv:hep-ph/0412203]; and references therein.
- [32] D. A. Dicus and H. J. He, *Scales of Fermion Mass Generation and Electroweak Symmetry Breaking*, Phys. Rev. D **71** (2005) 093009 [arXiv:hep-ph/0409131]; *Scales of Mass Generation for Quarks, Leptons and Majorana Neutrinos*, Phys. Rev. Lett. **94** (2005) 221802 [arXiv:hep-ph/0502178]; and references therein.
- [33] H. J. He and Z. Z. Xianyu, *Spontaneous Spacetime Reduction and Unitary Weak Boson Scattering at the LHC*, Phys. Lett. B **720** (2013) 142 [arXiv:1301.4570]; *Unitary Standard Model from Spontaneous Dimensional Reduction and Weak Boson Scattering at the LHC*, Eur. Phys. J. Plus **128** (2013) 40 [arXiv:1112.1028].
- [34] H. J. He, Y. P. Kuang, C. P. Yuan, B. Zhang, *Anomalous Gauge Interactions of Higgs Boson: Precision Constraints and Weak Boson Scatterings*, Phys. Lett. B **554** (2003) 64 [hep-ph/0211229]; and *W⁺W⁺ Scattering as a Sensitive Test of Anomalous Gauge Couplings of Higgs Boson at the LHC*, arXiv:hep-ph/0401209, in proceedings of the “Workshop on Physics at TeV Colliders”, Les Houches, France, May 26–June 6, 2003. For some recent studies, T. Han, D. Krohn, L. T. Wang and W. Zhu, *New physics signals in longitudinal gauge boson scattering at the LHC*, JHEP **1003** (2010) 082 [arXiv:0911.3656]; Y. Cui and Z. Han, *New light on WW scattering at the LHC with W jet tagging*, Phys. Rev. D **89** (2014) 015019 [arXiv:1304.4599]; H. Murayama, V. Rentala, and J. Shu, *Disentangling strong dynamics through quantum interferometry*, arXiv:1401.3761; and references therein.
- [35] P. Ade *et al.*, [Planck Collaboration], *Planck 2013 Results, XXII: Constraints on Inflation*, arXiv:1303.5082 [astro-ph.CO].
- [36] E.g., D. S. Salopek, J. R. Bond and J. M. Bardeen, *Designing Density Fluctuation Spectra in Inflation*, Phys. Rev. D **40** (1989) 1753; B. L. Spokoiny, *Inflation and Generation of Perturbations in Broken Symmetric Theory of Gravity*, Phys. Lett. B **147** (1984) 39; R. Fakir and W. G. Unruh, *Improvement on Cosmological Chaotic Inflation through Nonminimal Coupling*, Phys. Rev. D **41** (1990) 1783; *Induced Gravity Inflation*, Phys. Rev. D **41** (1990) 1792; J. Cervantes-Cota and H. Dehnen, *Induced Gravity Inflation in the Standard Model of Particle Physics*, Nucl. Phys. B **442** (1995) 391 [astro-ph/9505069]; *Induced Gravity Inflation in the SU(5) GUT*, Phys. Rev. D **51** (1995) 395 [astro-ph/9412032]; and references therein.
- [37] C. P. Burgess, S. P. Patil, and M. Trott, *On the Predictiveness of Single-Field Inflationary Models*, arXiv:1402.1476 [hep-ph].